Mitigation of Torsional Vibrations in Drilling Systems: A Robust Control Approach

Thijs Vromen, Cam-Hing Dai, Nathan van de Wouw, *Member, IEEE*, Tom Oomen, *Member, IEEE*, Patricia Astrid, *Member, IEEE*, Apostolos Doris, and Henk Nijmeijer, *Fellow, IEEE*

***Abstract*— Stick-slip vibrations decrease the performance, reliability, and fail safety of drilling systems. The aim of this paper is to design a robust output-feedback control approach to eliminate torsional stick-slip vibrations in drilling systems. Current industrial controllers regularly fail to eliminate stick-slip vibrations, especially when multiple torsional flexibility modes play a role in the onset of stick-slip vibrations. As a basis for controller synthesis, a multimodal model of the torsional dynamics for a real drill-string system is employed. The proposed controller design strategy is based on skewed-μ DK iteration and aims at optimizing the robustness with respect to uncertainty in the nonlinear bit–rock interaction. Moreover, a closed-loop stability analysis for the nonlinear drill-string model is provided. This controller design strategy offers several benefits compared with existing controllers. First, only surface measurements are employed, therewith avoiding the need for down-hole measurements. Second, multimodal drill-string dynamics are effectively dealt with in ways inaccessible to state-of-practice controllers. Third, robustness with respect to uncertainties in the bit–rock interaction is explicitly provided and closed-loop performance specifications are included in the controller design. Case study results confirm that stick-slip vibrations are indeed eliminated in realistic drilling scenarios using the designed controller in which state-of-practice controllers fail to achieve this.**

***Index Terms*— μ-synthesis, drilling systems, output feedback, robust control, stick-slip oscillations.**

I. Introduction

EFFICIENCY, reliability, and safety are important aspects in the drilling of deep wells for the exploration and production of oil, gas, mineral resources, and geo-thermal energy. Deep and curved borehole geometries need to be drilled to reach hydrocarbon reservoirs and extract these natural resources. For these borehole geometries, complicated bottom-hole-assemblies (BHAs) are required that can include mud motors, rotary steerable systems, or turbines. In combination with such BHAs, drill strings of several kilometers in length are used to transmit the axial force and torque necessary to drill the rock formations. These drill-string systems are known to exhibit different types of self-excited vibrations, which decrease the drilling efficiency, accelerate bit wear, and may cause drill-string failure due to fatigue (see [1]–[4]). The focus of this paper is on the aspect of mitigation of torsional stick-slip vibrations by developing a model-based design approach for robust linear output-feedback controllers.

Different approaches to model the drill-string dynamics can be found in the literature. The differences between those approaches involve two key aspects, namely, modeling of the drill string and modeling of the bit–rock interaction. Both aspects are concisely discussed, starting with the bit–rock interaction, and the approach we have taken is motivated. Note that the focus of this paper is on controller design and therefore drill-string modeling is only briefly discussed. Most controller designs presented in the literature rely on 1- or 2-degree-of-freedom (DOF) models for the torsional dynamics only (see [5]–[7]). In these models, it is generally assumed that the resisting torque at the bit–rock interface can be modeled as a frictional contact with a velocity-weakening effect. In fact, modeling of the coupled axial and torsional dynamics, as, for example, in [8]–[10], shows that the velocity-weakening effect in the torque-on-bit (TOB) is a consequence of the drilling dynamics [8], [11]. The fact that such coupling effectively leads to a velocity-weakening effect of the TOB (see [8], [12]) motivates to adopt a modeling-for-control approach for drill-string dynamics involving the torsional dynamics only and incorporating a velocity-weakening bit–rock interaction law.

The second key aspect involves the modeling approach for the drill string itself. An extensive overview of modeling of oil well drilling systems from a vibration perspective can be found in [13]. In contrast to other studies (see [5]–[7], [12], [14], [15]), we use a multimodal finite-element method (FEM) model representation of the torsional dynamics, as also pursued in [4], [11], [16], and [17] specifically for horizontal drilling scenarios. A FEM model representation is used because field observations have revealed that multiple

Manuscript received January 11, 2017; revised July 23, 2017; accepted September 6, 2017. Date of publication November 2, 2017; date of current version December 12, 2018. Manuscript received in final form October 3, 2017. This work was supported by Shell Global Solutions International. Recommended by Associate Editor A. Pavlov. *(Corresponding author: Thijs Vromen.)*

T. Vromen, C.-H. Dai, T. Oomen, and H. Nijmeijer are with the Department of Mechanical Engineering, Eindhoven University of Technology, 5600 MB Eindhoven, The Netherlands (e-mail: t.g.m.vromen@tue.nl; c.h.dai@student.tue.nl; t.a.e.oomen@tue.nl; h.nijmeijer@tue.nl).

N. van de Wouw is with the Department of Mechanical Engineering, Eindhoven University of Technology, 5600 MB Eindhoven, The Netherlands, and also with the Delft Center for Systems and Control, Delft University of Technology, 2628 CD Delft, The Netherlands, and also with the Department of Civil, Environmental and Geo-Engineering, University of Minnesota, Minneapolis, MN 55455 USA (e-mail: n.v.d.wouw@tue.nl).

P. Astrid is with the Shell Global Solutions International B.V., 2288 GS Rijswijk, The Netherlands (e-mail: patricia.astrid@shell.com).

A. Doris is with Nederlandse Aardolie Maatschappij B.V., 9405 TA Assen, The Netherlands (e-mail: apostolos.doris@shell.com).

Color versions of one or more of the figures in this paper are available online at http://ieeexplore.ieee.org.

Digital Object Identifier 10.1109/TCST.2017.2762645

torsional resonance modes play a role in the onset of stick-slip oscillations [18], [19]. A different modeling approach is taken in [11] and [20]–[25], where infinite-dimensional models, i.e., formulated in terms of partial or delay differential equations, are considered. Discretizations of such infinite-dimensional models (see [26], [27]) result in a lumped parameter model, based on a finite-element representation of the drill-string dynamics; this approach is also taken in this paper. Summarizing, we employ a (multimodal) FEM model of the drill-string dynamics involving the torsional dynamics only and a velocity-weakening bit–rock interaction law to support a model-based controller design strategy.

Controllers for drilling systems aim at drill-string rotation at a constant angular velocity and the mitigation of torsional (stick-slip) vibrations. Moreover, the following control specifications are essential. First, only surface measurements can be used for feedback, because down-hole measurements for real-time control purposes are not available in practice, due to limitations on the sampling rate, time delay of the measurements, and/or the high costs involved. Second, the controller should be able to cope with dynamics related to multiple torsional flexibility modes. Third, robustness with respect to uncertainty in the bit-rock interaction has to be guaranteed (as it depends on uncertain factors, such as rock properties and bit wear). Fourth, control performance specifications need to be taken into account in the controller design, to achieve robust performance in the presence of measurement noise and actuator constraints.

Several approaches have been developed that address one or more of these requirements. For instance, the well-known and state-of-practice *soft torque rotary system* [15], which uses both torque feedback and (top drive) velocity feedback, only to damp the first torsional mode. The same objective is set in [5], where a PI controller to damp the first resonance mode based on feedback of the top drive velocity only is used. Other control methods, including torsional rectification [25], observer-based output feedback [7], [28], [29], feedback linearization [30], impedance matching [31], adaptive output-feedback for infinite dimensional drill-string models [23], backstepping control [32], sliding mode control [33], model predictive control [34], weight-on-bit (WOB) control [35], and robust control [6], [14], have been developed. A nonlinear observer-based approach for stick-slip mitigation is presented in [29], which uses a similar approach to model the drilling dynamics as employed in this paper. Such an observer-based state-feedback approach requires information about the bit–rock interaction in the observer, which is typically not available in practice. Moreover, control performance specifications, e.g., on noise sensitivity or actuator constraints, are not taken into account in the controller design and only low-order drill-string models can be used as a basis for the linear matrix inequality-based design in [29]. Wave-based approaches for multimodal vibration damping, such as presented in [25], [26], and [31], are designed to cope with the dynamics related to multiple torsional flexibility modes. However, to the best of our knowledge, a stability analysis proving robust (local) asymptotic stability of the drill-string dynamics in closed loop with such a controller and in the presence of a (uncertain) nonlinear bit–rock interaction has not been presented yet. Moreover, it is not possible to take control performance specifications directly into account in the controller design with these methods. Another important difference with the impedance matching method (see [31]) is the fact that this method is based on matching the impedance of the top part of the drill string (i.e., close to the top drive) rather than matching the impedance of the whole drill string including, e.g., BHA, tool connectors, and the bit–rock interaction. The method proposed in this paper takes the dynamics (most dominant modes) of the entire drill string, including BHA, into account for the controller design. In summary, none of the above approaches addresses all the four requirements in the previous paragraph simultaneously.

To satisfy all the requirements mentioned above, a robust control approach is particularly suitable, since robustness with respect to uncertainty of the system dynamics can be taken into account in the design. For drill-string models focusing on torsional dynamics, the nonlinear bit–rock interaction model is often difficult to determine and is therefore considered as a particularly uncertain factor. Despite the fact that [6] and [14] use such a robust control approach, also these approaches do not satisfy all requirements mentioned above. As mentioned before, multiple torsional flexibility modes are important in the onset of stick-slip vibrations, whereas the 2-DOF models employed in [6] and [14] take only the first flexibility mode into account. Moreover, the designed controllers rely on down-hole measurements to assess the twist of the drill string. In this paper, we propose a robust controller design technique on the basis of a multimodal FEM drill-string model that relies on surface measurements only.

The main contribution of this paper is the design of a robust output-feedback controller synthesis methodology to eliminate stick-slip vibrations with the following advantages over existing controllers: 1) usage of surface measurements only; 2) effectively dealing with the multimodal nature of the drill-string dynamics while guaranteeing local stability of the desired setpoint; 3) optimization of the robustness with respect to uncertainty in the bit–rock interaction; and 4) integration of key control performance specifications in the design approach. Preliminary results of this controller design strategy applied to a simplified 4-DOF drill-string model have been presented in [36]. Additional contributions of this paper are the application of the controller design methodology to a full-scale finite-element model representing a real drilling system. Additionally, key robustness aspects of the closed-loop system are investigated in detail. The following robustness aspects are key in the scope of practical applications and are extensively studied in this paper: robustness with respect to changes in the bit–rock interaction characteristic, increasing length of the drill-string, and different desired angular velocities (i.e., increased operating envelope).

This paper is organized as follows. In Section II, the control problem is formulated. Subsequently, in Section III, the drill-string model based on a finite-element model of a real-life drill-string system is introduced. Next, in Section IV, the design of an output-feedback controller based on skewed-μ DK iteration is proposed and the controller synthesis by

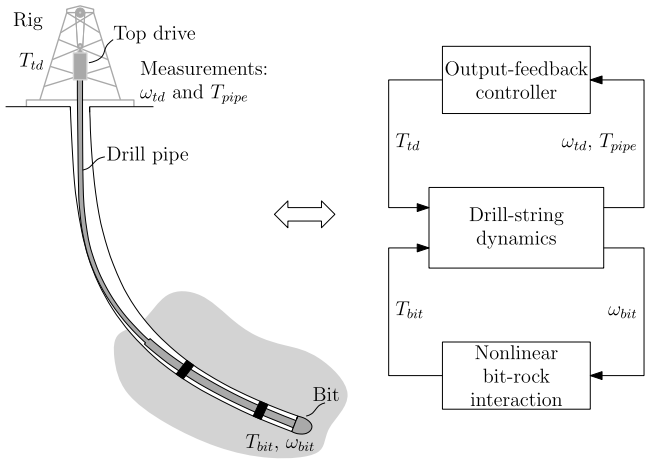

Fig. 1. Schematic of a drilling system and the corresponding block diagram for controller design.

weighting filter design is treated in Section V. In Section VI, simulation results illustrating the effectiveness of the proposed approach are presented and compared with the results obtained using an industrial controller. Next, in Section VII, the robustness of the controller is investigated by means of several case studies involving realistic drilling scenarios. Finally, the results are summarized in Section VIII.

II. Control Problem Formulation

A. System Description

A drilling system, as schematically shown in Fig. 1, can be roughly divided in three parts; a drill bit at the bottom of the borehole for rock cutting, a drill string to transmit torque to the bit, and a top drive at surface to drive the system. The top drive torque to drive the system is given by T_{td}. As mentioned in Section I, one of the key aspects for controllers to be used in practice is the usage of surface measurements only. These measurements are indicated by the top drive velocity ω_{td} and the pipe torque T_{pipe}, which is defined as the torque in the drill string directly below the top drive. The bit–rock interaction, which plays an important role in the existence of stick-slip vibrations in drilling system, is described by a nonlinear relation between the bit angular velocity ω_{bit} and the torque at the bit–rock interface T_{bit}.

On the right side of Fig. 1, a block diagram representation of the (closed-loop) drill-string system is given. In this block diagram, the drill-string dynamics and the nonlinear bit–rock interaction describe the nonlinear open-loop drill-string dynamics; the drill-string model is discussed in more detail in Section III-A. The upper block in the block diagram indicates the output-feedback controller to be designed; the objectives for this controller are summarized in Section II-B.

B. Controller Objectives

In this section, we formulate the control problem and specify the controller objectives. The desired operation of the drill-string system is a constant (positive) angular velocity ω_{eq} for the entire drill string. Thus, the objective is to regulate the nonlinear drill-string system to this setpoint by means of an output-feedback controller (and a constant feedforward torque). As briefly mentioned in Section I, the controller should do the following:

1) ensure a constant angular velocity ω_{eq} for the entire drill string using surface measurements only, therewith eliminating stick-slip vibrations, i.e., locally stabilize the constant rotational velocity ω_{eq} of the drill string;
2) ensure robustness with respect to uncertainty in the nonlinear bit–rock interaction, by taking the bit–rock interaction into account as uncertainty (see Section III-B for more details) and optimize the robustness with respect to this uncertainty;
3) guarantee the satisfaction of prespecified closed-loop performance specifications, in particular on measurement noise sensitivity, and limitation of the control action such that top drive limitations can be satisfied;
4) guarantee stability and performance in the presence of multiple flexibility modes dominating the torsional dynamics.

III. Modeling for Control

A FEM model of a real drilling system is used as basis for controller design. The model is based on an offshore jack-up drilling rig to reach reservoir sections at depths of more than 6000 m and with an inclination angle up to 60°, resulting in significant resistive torques along the drill string. The rig is equipped with an AC top drive and fitted with a modern SoftTorque system [5], [19], [37]. When drilling those deep deviated wells, stick-slip vibrations have been observed in the field for this drilling system [38]. This motivates the use of this drill-string model, representing a real-life and challenging scenario, as a basis for the development of a novel controller design methodology.

A. Drill-String Dynamics Model

The FEM is used to construct a multimodal torsional drill-string model. The element at the top is a rotational inertia to model the top drive inertia; the subsequent elements are equivalent pipe sections based on the dimensions and material properties of the drill string (see [39] for more details). The resulting model is written as

$$M\ddot{\theta} + D\dot{\theta} + K_t\theta_d = S_w T_w(\dot{\theta}) + S_b T_{\text{bit}}(\dot{\theta}_1) + S_t T_{\text{td}} \quad (1)$$

with the coordinates $\theta \in \mathbb{R}^m$ with m the number of elements in the FEM model, the top drive motor torque input $T_{\text{td}} \in \mathbb{R}$ being the control input, the bit–rock interaction torque $T_{\text{bit}} \in \mathbb{R}$, and the interaction torques $T_w \in \mathbb{R}^{m-1}$ between the borehole and the drill string acting on the nodes of the FEM model. The terms T_{bit} and T_w describe the boundary conditions at the bit and along the drill string, respectively; the boundary condition at the top is defined by T_{td} and given by the controller that is designed and discussed in Sections IV and V in more detail. The coordinates θ represent the angular displacements of the nodes of the finite-element representation. Next, we define the difference in angular position between adjacent nodes as follows: $\theta_d := [\theta_1 - \theta_2 \;\; \theta_2 - \theta_3 \;\; \cdots \;\; \theta_{m-1} - \theta_m]^\top$.

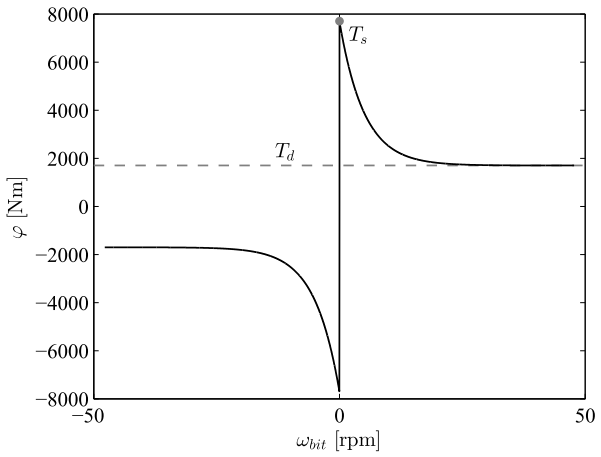

Fig. 2. Bit–rock interaction model.

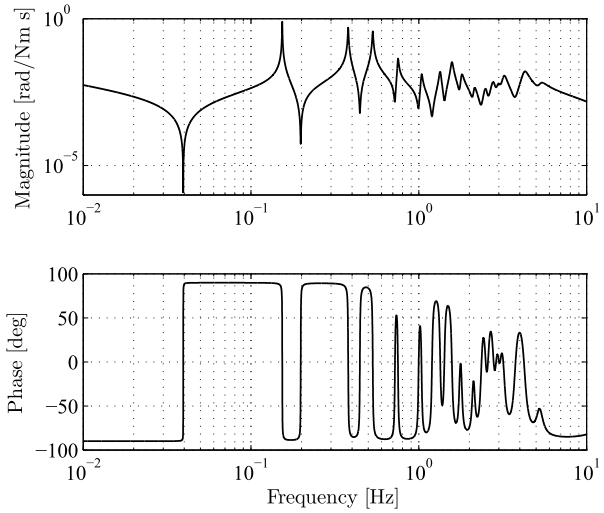

Fig. 3. Frequency response function of the 18-DOF model from bit torque T_{bit} to bit velocity ω_{bit}, i.e., bit mobility.

In (1), the mass, damping, and "stiffness" matrices are, respectively, given by $M \in \mathbb{R}^{m\times m}$, $D \in \mathbb{R}^{m\times m}$, and $K_t \in \mathbb{R}^{m\times m-1}$, and the matrices $S_w \in \mathbb{R}^{m\times m-1}$, $S_b \in \mathbb{R}^{m\times 1}$, and $S_t \in \mathbb{R}^{m\times 1}$ represent the generalized force directions of the interaction torques, the bit torque, and the input torque, respectively. These matrices are explicated in the Appendix for an 18-DOF finite-element model that has been validated with field data (see [39]). The coordinates θ are chosen such that the first element (θ_1) describes the rotation of the bit and the last element (θ_m) the rotation of the top drive at surface. The interaction between the borehole and the drill string is modeled as Coulomb friction, that is

$$T_{w,i} \in T_i \ \text{Sign}(\dot{\theta}_i), \quad \text{for } i = 2, \ldots, m \tag{2}$$

with T_i representing the amount of friction at each element and the set-valued sign function defined as

$$\text{Sign}(y) \triangleq \begin{cases} -1, & y < 0 \\ [-1, 1], & y = 0 \\ 1, & y > 0. \end{cases} \tag{3}$$

The amount of friction at each node is such that it represents the interaction torque along the corresponding section of the drill string, depending on depth and shape (i.e., inclination) of the borehole. The bit–rock interaction model, including the velocity-weakening effect, is given by

$$T_{\text{bit}}(\dot{\theta}_1) \in \text{Sign}(\dot{\theta}_1)(T_d + (T_s - T_d)e^{-v_d|\dot{\theta}_1|}) \tag{4}$$

with T_s the static torque, T_d the dynamic torque, and $v_d := (30/N_d\pi)$ indicating the decrease from static to dynamic torque. For this model, the parameters are identified such that a match between the simulation results and the (surface) field data is obtained (see [39]). The parameter values are given by $T_s = 7700$ Nm, $T_d = 1700$ Nm, and $N_d = 5$ r/min, and the resulting bit–rock interaction model is shown in Fig. 2. The drill-string-borehole interaction torques $T_{w,i}(\dot{\theta}_i)$, $i = 2, \ldots, m$, are defined by $\phi(q_2) := [T_{w,2}(\dot{\theta}_2) \ \cdots \ T_{w,m}(\dot{\theta}_m)]^\top$ with $q_2 := [\dot{\theta}_2 \ \cdots \ \dot{\theta}_m]^\top$ and the interaction torque at the bit–rock interface is written as $\varphi(q) := T_{\text{bit}}(\dot{\theta}_1)$. The resulting equations of motion are written in first-order (Lur'e-type) state-space form

$$\begin{aligned} \dot{x} &= Ax + Gv + G_2 v_2 + Bu_t \\ q &= Hx \\ q_2 &= H_2 x \\ y &= Cx \\ v &\in -\varphi(q) \\ v_2 &\in -\phi(q_2). \end{aligned} \tag{5}$$

Herein, $x := [\theta_d \ \dot{\theta}]^\top \in \mathbb{R}^{2m-1}$ is the state. The top drive velocity and bit velocity are defined as $\omega_{\text{td}} := \dot{\theta}_m$ and $\omega_{\text{bit}} = q := \dot{\theta}_1$, respectively. The available measurements are the top drive velocity ω_{td} and the pipe torque T_{pipe}. Therefore, the measured output is defined as $y := [\omega_{\text{td}} \ T_{\text{pipe}}]^\top \in \mathbb{R}^2$ and the control input is given by $u_t := T_{\text{td}} \in \mathbb{R}$. The matrices A, B, C, G, G_2, H, and H_2 in (5), with appropriate dimensions, are given by

$$\begin{aligned} A &= \begin{bmatrix} O_{m-1\times m-1} & a \\ -M^{-1}K_t & -M^{-1}D \end{bmatrix} \\ a &= \begin{bmatrix} 1 & -1 & 0 & \cdots & 0 \\ 0 & \ddots & \ddots & \ddots & \vdots \\ \vdots & \ddots & \ddots & \ddots & 0 \\ 0 & \cdots & 0 & 1 & -1 \end{bmatrix} \\ B &= \begin{bmatrix} O_{m-1\times 1} \\ M^{-1}S_t \end{bmatrix}, \quad C = \begin{bmatrix} O_{1\times 2m-2} & 1 \\ J_{\text{td}}M^{-1}K_t & J_{\text{td}}M^{-1}D \end{bmatrix} \\ G &= \begin{bmatrix} O_{m-1\times 1} \\ M^{-1}S_b \end{bmatrix}, \quad G_2 = \begin{bmatrix} O_{m-1\times m-1} \\ M^{-1}S_w \end{bmatrix} \\ H &= \begin{bmatrix} O_{1\times m-1} & 1 & O_{1\times m-1} \end{bmatrix}, \quad H_2 = \begin{bmatrix} O_{m-1\times m} & I_{m-1} \end{bmatrix} \end{aligned}$$

with J_{td} the top drive inertia, I_k the k-by-k identity matrix and $O_{k\times l}$ a k-by-l matrix with all zero entries.

One of the most relevant frequency response functions of the linear part of the dynamics (5) is shown in Fig. 3 for $m = 18$. This frequency response function is called the bit mobility, as it describes the transfer from bit torque to bit velocity.

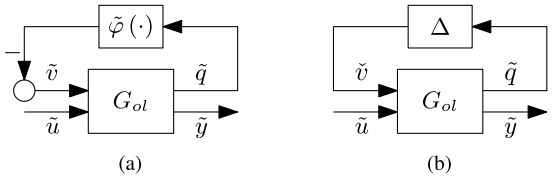

Fig. 4. Block diagram of the (a) system dynamics (7) in Lur'e type form and (b) linear dynamics $G_{\rm ol}$ with (complex) model uncertainty Δ.

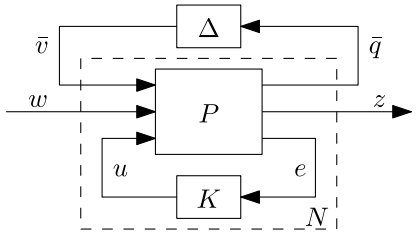

Fig. 5. General control configuration with uncertainty block Δ.

The bit-mobility gives an indication of the dominant resonance modes in the onset of stick-slip vibrations. Namely, it represents the input–output dynamics, which, in 'closed loop' with the nonlinear bit–rock interaction law, is responsible for the presence (or not) of torsional instabilities and stick-slip vibrations. Therefore, damping/suppression of the resonance modes in the bit mobility plays an important role in the controller design methodology in Section IV.

B. Model in Perturbation Coordinates

To facilitate controller synthesis, the drill-string dynamics (5) are rewritten. The desired constant angular velocity $\omega_{\rm eq}$ is associated with a desired equilibrium $x_{\rm eq}$ for the state of the system. To ensure that $x_{\rm eq}$ is indeed an equilibrium of the closed-loop system, the control input $u_t = u_c + \tilde{u}$ is decomposed in a constant feedforward torque u_c (inducing $x_{\rm eq}$) and the feedback control input $\tilde{u}$. For the purpose of feedforward design, we assume that $\omega_i > 0$, for $i = 2, \ldots, m$; then it follows from (2) that the resistive torques along the drill string (ϕ_i) are constant. Hence, ϕ is constant and can be compensated for by u_c. The (constant) equilibrium $x_{\rm eq}$ and feedforward torque u_c can be obtained from the equilibrium inclusion of system (5)

$$Ax_{\rm eq} - G\varphi(Hx_{\rm eq}) - G_2\phi(H_2x_{\rm eq}) + Bu_c \ni 0. \tag{6}$$

Next, let $\xi := x - x_{\rm eq}$ represent the state error. Moreover, we apply a linear loop transformation such that the slope of a transformed nonlinearity $\tilde{\varphi}(q)$ [associated to $\varphi(q)$ through the loop transformation] is equal to zero at the desired equilibrium velocity, i.e., $(\partial\tilde{\varphi}/\partial q)|_{q=\omega_{\rm eq}} = 0$. This results in the following state-space representation of the transformed drill-string dynamics in perturbation coordinates:

$$\dot{\xi} = A_t\xi + B\tilde{u} + G\tilde{v} \tag{7a}$$

$$\tilde{q} = H\xi \tag{7b}$$

$$\tilde{y} = C\xi \tag{7c}$$

$$\tilde{v} \in -\tilde{\varphi}(\tilde{q}) \tag{7d}$$

with $A_t := A + \delta GH$, $\delta = -(\partial\varphi/\partial q)|_{q=\omega_{\rm eq}} > 0$, $\tilde{y} := y - Cx_{\rm eq}$, $\tilde{q} := q - Hx_{\rm eq}$, $\tilde{\varphi}(\tilde{q}) := \varphi(\tilde{q} + Hx_{\rm eq}) - \varphi(Hx_{\rm eq}) + \delta\tilde{q}$, and $\tilde{v} := v - v_{\rm eq} - \delta\tilde{q}$. The dynamics in (7) represents a Lur'e-type system [see Fig. 4(a)] with the linear dynamics $G_{\rm ol}$ [(7a)–(7c)], having inputs $\tilde{u}$ and $\tilde{v}$ and outputs $\tilde{y}$ and $\tilde{q}$, and the nonlinearity $\tilde{\varphi}$ in the feedback loop. The open-loop transfer function $G_{\rm ol}(s)$, $s \in \mathbb{C}$, characterizes the linear input–output dynamics through

$$\begin{bmatrix}\tilde{q}(s)\\ \tilde{y}(s)\end{bmatrix} := G_{\rm ol}(s)\begin{bmatrix}\tilde{v}(s)\\ \tilde{u}(s)\end{bmatrix} = \begin{bmatrix}g_{11}(s) & g_{12}(s)\\ g_{21}(s) & g_{22}(s)\end{bmatrix}\begin{bmatrix}\tilde{v}(s)\\ \tilde{u}(s)\end{bmatrix}. \tag{8}$$

Note that this representation corresponds to the block diagram in Fig. 1 (although here formulated in perturbation coordinates) with, respectively, $\tilde{y}$ and $\tilde{u}$ the input and output for the controller to be designed, $G_{\rm ol}$ the (linear) drill-string dynamics, and $\tilde{\varphi}$ the nonlinear bit–rock interaction.

In the context of the second controller objective (Section II-B), we model the nonlinearity $\tilde{\varphi}$ [Fig. 4(a)] by an uncertainty Δ [Fig. 4(b)]. This model formulation is used in the controller design approach developed in Section IV. Note that $\tilde{\varphi}$ describes a nonlinear mapping from $\tilde{q}$ to $\tilde{v}$, while the uncertainty Δ is assumed to be a (complex) linear time-invariant (LTI) uncertainty (with output $\check{v}$). This means that, for example, stability of the closed-loop system with uncertainty Δ does not directly imply stability for the closed-loop system with nonlinearity $\tilde{\varphi}$. Nevertheless, the model in Fig. 4(b) is used as a basis for controller synthesis in Section IV. Subsequently, the stability of the nonlinear closed-loop system is analyzed in detail in Section IV-D.

IV. Controller Design Methodology

In this section, we present a robust control design approach based on skewed-μ DK iteration. This technique combines several concepts from robust control theory to design a linear controller that achieves robust stability and performance of a system with model uncertainties [40].

Robust control methods focus on the design of controllers while system uncertainties are explicitly taken into account in the design. The general control configuration for a (LTI) plant P with an uncertainty Δ and (LTI) controller K is shown in Fig. 5, where e is the error in the measured output, u the control output, and w and z represent the (weighted) exogenous inputs and outputs. This structure is similar to the block diagram in Fig. 4(a) with $\bar{v}$ and $\bar{q}$ weighted representations of $\check{v}$ and $\tilde{q}$ (see Section IV-B) and in addition the controller K. The system P, in Fig. 5, is described by

$$\begin{bmatrix}\bar{q}\\ z\\ e\end{bmatrix} = \begin{bmatrix}P_{11} & P_{12} & P_{13}\\ P_{21} & P_{22} & P_{23}\\ P_{31} & P_{32} & P_{33}\end{bmatrix}\begin{bmatrix}\bar{v}\\ w\\ u\end{bmatrix}. \tag{9}$$

The system $N := F_l(P, K)$ is defined as the lower linear fractional transformation (LFT) of the plant P with the controller K, that is

$$N = \begin{bmatrix}P_{11} & P_{12}\\ P_{21} & P_{22}\end{bmatrix} + \begin{bmatrix}P_{13}\\ P_{23}\end{bmatrix}K(I - P_{33}K)^{-1}[P_{31}\ \ P_{32}].$$

With the introduction of the controller K, we can also introduce the closed-loop bit-mobility function. The closed-loop bit-mobility transfer function $G_{\rm cl}$ from the input $\tilde{v}$ to the

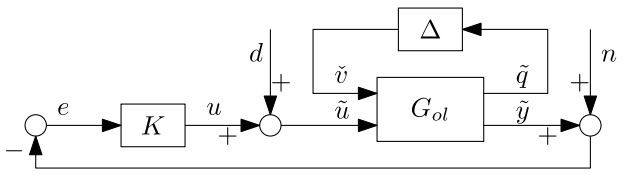

Fig. 6. Linear drill-string dynamics $G_{\rm ol}$ in closed loop with the controller K and including model uncertainty Δ.

output $\tilde{q}$, of system (7) with controller K, is defined by

$$G_{\rm cl} := g_{11} - g_{12}K(I + g_{22}K)^{-1}g_{21}. \tag{10}$$

As mentioned in Section III, this bit mobility plays an important role in the stability of the closed-loop system (see Section IV-D for the role of $G_{\rm cl}$ in the scope of a nonlinear stability analysis) and is therefore important in the controller design methodology.

A. Nominal Stability and Nominal Performance

As mentioned in Section II-B, the controller design aims at stability, performance, and robustness for the uncertainty Δ. In this section, the focus is on the first two aspects. Robustness is considered in Section IV-B. Based on the system representation in Fig. 4(b), the closed-loop system of the linear drill-string dynamics $G_{\rm ol}$ in feedback with the linear dynamic controller K to be designed is shown in Fig. 6. In this representation, additional inputs n and d are introduced, representing measurement noise and actuator noise, respectively.

Consider the system without uncertainty given by

$$\begin{bmatrix} z \\ e \end{bmatrix} := P_{\rm sub}\begin{bmatrix} w \\ u \end{bmatrix} = \begin{bmatrix} P_{22} & P_{23} \\ P_{32} & P_{33} \end{bmatrix}\begin{bmatrix} w \\ u \end{bmatrix} \tag{11}$$

with w and z weighted versions of $\underline{w} := [n\ d]^\top$ and $\underline{z} := [e\ u]^\top$, respectively. The weighted inputs and outputs are discussed in more detail in Section IV-B. Moreover, define the lower LFT of $P_{\rm sub}$ with the controller K, that is, $N_{22} := F_l(P_{\rm sub}, K)$. Next, the concept of nominal performance is defined as follows: for a system without uncertainty Δ, the closed-loop system $N_{22} = F_l(P_{\rm sub}, K)$ is internally stable and the $\mathcal{H}_\infty$-norm of this system (from w to z) is smaller than one, that is:

$$\|N_{22}\|_\infty = \sup_\omega \bar{\sigma}\left(F_l(P_{\rm sub}, K)\right) < 1 \tag{12}$$

where we used the definition of the $\mathcal{H}_\infty$-norm $\|H(s)\|_\infty := \operatorname{ess\,sup}_{\omega\in\mathbb{R}} \bar{\sigma}(H(j\omega))$. This means that nominal performance can be achieved by solving the "standard" $\mathcal{H}_\infty$ optimal control problem, where the aim is to find the internally stabilizing controller K that minimizes $\|F_l(P_{\rm sub}, K)\|_\infty$ (see [40] for details). Internal stability of the closed loop can be guaranteed by a proper choice of the inputs w and outputs z. As proved in [41, Section 5.3], by choosing w and z as defined earlier, the $\mathcal{H}_\infty$ controller synthesis guarantees internal stability of the closed-loop system. Specification of the weighting filters is treated in more detail in Section IV-B. Moreover, the system *with* uncertainty is addressed in Section IV-B, leading to the concept of robust performance.

B. Alternative Robust Performance

Robust performance means that the stability and performance objective, addressed in Section IV-A, is achieved for all possible models in the uncertainty set $\mathbf{\Delta}$ [40]. Standard robust performance techniques typically aim at optimizing the performance for all possible plants in the uncertainty set. In contrast, we aim to optimize the robustness with respect to the uncertainty while still guaranteeing internal stability and satisfaction of given performance objectives. This is what we call *alternative robust performance*. In the drilling context, this means that for example, a (fixed) bound on the control action should be satisfied (see the third controller objective in Section II-B), while the robustness with respect to the nonlinear bit–rock interaction is optimized (as specified in the second controller objective).

Consider the system P in Fig. 5, including the uncertainty block Δ. The input–output pair $\bar{v}$, $\bar{q}$ is related to this uncertainty block and the (weighted) closed-loop transfer function $N(s) = F_l(P, K)$ is given by

$$\begin{bmatrix} \bar{q} \\ w \end{bmatrix} = N\begin{bmatrix} \bar{v} \\ z \end{bmatrix} = F_l(P, K)\begin{bmatrix} \bar{v} \\ z \end{bmatrix}. \tag{13}$$

Robust stability is obtained by designing a controller K such that the system N is internally stable and the upper LFT, $F := F_u(N, \Delta)$, is stable for all $\Delta \in \mathbf{\Delta}$. Herein, the uncertainty set $\mathbf{\Delta}$ is a norm-bounded subset of $\mathcal{H}_\infty$,[1] i.e., $\mathbf{\Delta} = \{\Delta \in \mathcal{RH}_\infty \,|\, \|\Delta\|_\infty < 1\}$. The aim is to find a stabilizing controller that also meets certain performance specifications. Therefore, we use the same approach as in [40, Sec. 8.10] and consider the fictitious 'uncertainty' Δ_P. The uncertainty Δ_P is a complex unstructured uncertainty block that represents the $\mathcal{H}_\infty$ performance specifications. Moreover, note that $\Delta_P \in \mathbf{\Delta}_P$, with $\mathbf{\Delta}_P = \{\Delta_P \in \mathcal{RH}_\infty \,|\, \|\Delta_P\|_\infty \le 1\}$. The result given in [41, Th. 11.8] states that a robust performance problem is equivalent to a robust stability problem with the augmented uncertainty

$$\hat{\Delta} = \begin{bmatrix} \Delta & 0 & 0 \\ 0 & & \\ 0 & & \Delta_P \end{bmatrix} \tag{14}$$

with $\hat{\Delta}$ a block-diagonal matrix. In other words, both the performance specifications and uncertainty are taken into account in a similar fashion. Moreover, $\hat{\mathbf{\Delta}}$ is the uncertainty set with the structure as given in (14) and any $\Delta \in \mathbf{\Delta}$ and $\Delta_P \in \mathbf{\Delta}_P$. The robust performance condition can now be formulated as follows:

$$\mu_{\hat{\mathbf{\Delta}}}(N(j\omega)) \le 1, \quad \forall\omega \tag{15}$$

where $\mu_{\hat{\mathbf{\Delta}}}$ is the structured singular value with respect to $\hat{\mathbf{\Delta}}$. The structured singular value is defined as the real nonnegative function

$$\mu_{\hat{\mathbf{\Delta}}}(N) = \frac{1}{\bar{k}_m}, \quad \bar{k}_m = \min\{k_m \,|\, \det(I - k_m N\hat{\Delta}) = 0\} \tag{16}$$

with complex matrix N and block-diagonal uncertainty $\hat{\Delta}$.

[1] $\mathcal{H}_\infty$ is a (closed) Banach space of matrix-valued functions that are analytic in the open right-half plane and bounded on the imaginary axis. The real rational subspace of $\mathcal{H}_\infty$ is denoted by $\mathcal{RH}_\infty$, which consists of all proper and real rational stable transfer matrices [41, Sec. 4.3].

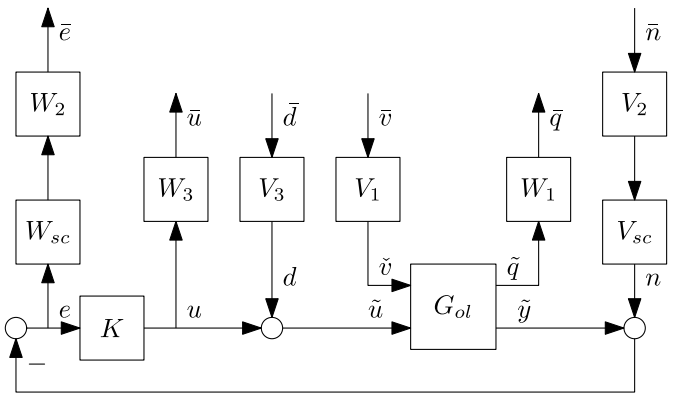

Fig. 7. Closed-loop system with weighting filters and scaling matrices.

To optimize the robustness with respect to the uncertainty Δ [i.e., part of $\hat{\Delta}$ in (14)], the skewed structured singular value μ^s can be used. The skewed structured singular value is used if some uncertainty blocks in $\hat{\Delta}$ are kept fixed (Δ_P in this case) to investigate how large another source of uncertainty (Δ in this case) can be, before robust stability/performance cannot be guaranteed anymore. In this case, we aim to optimize the robustness of the closed-loop system with respect to uncertainty Δ in the bit–rock interaction. Thus, we aim to obtain the largest uncertainty set Δ, given a fixed Δ_P (i.e., fixed performance specifications). Therefore, we introduce the matrix $K_m^s := \mathrm{diag}(k_m^s,\ I)$ and the skewed structured singular value $\mu_{\hat{\Delta}}^s(N)$ is defined as

$$\mu_{\hat{\mathbf{\Delta}}}^s(N) = \frac{1}{\bar{k}_m^s}, \quad \bar{k}_m^s = \min\left\{k_m^s \middle| \det\left(I - K_m^s N \hat{\Delta}\right) = 0\right\}. \quad (17)$$

Thus, the robust performance condition (15), with additional scaling (through K_m^s) in terms of the skewed structured singular value, is written as the *alternative* robust performance condition

$$\mu_{\hat{\mathbf{\Delta}}}^s(N(j\omega)) \leq 1, \quad \forall\omega. \quad (18)$$

To support controller design satisfying particular performance specifications, weighting filters, and scaling matrices are introduced in the loop in Fig. 6, as shown in Fig. 7. Those frequency-domain weighting filters allow us to specify the (inverse) maximum allowed magnitudes of the closed-loop transfer functions. Moreover, the scaling matrices are introduced to improve the numerical conditioning of the problem and to tune the desired bandwidth. The (weighted) generalized plant P with input weighting filters $V_i(s)$ and output weighting filters $W_i(s)$, with $i \in \{1, 2, 3\}$, and scaling matrices W_{sc} and V_{sc}, is specified by

$$\begin{bmatrix} \tilde{q} \\ \bar{e} \\ \bar{u} \\ e \end{bmatrix} = \underbrace{\begin{bmatrix} W_1 & 0 & 0 & 0 \\ 0 & W_2 W_{\mathrm{sc}} & 0 & 0 \\ 0 & 0 & W_3 & 0 \\ 0 & 0 & 0 & I_2 \end{bmatrix} \underline{P} \begin{bmatrix} V_1 & 0 & 0 & 0 \\ 0 & V_{\mathrm{sc}} V_2 & 0 & 0 \\ 0 & 0 & V_3 & 0 \\ 0 & 0 & 0 & 1 \end{bmatrix}}_{P} \begin{bmatrix} \tilde{v} \\ \bar{n} \\ \bar{d} \\ u \end{bmatrix}$$

where $\underline{P}(s)$ is the multiple-input and multiple-output transfer function of the unweighted system $\underline{P}$ with inputs $[\tilde{v}\ n\ d\ u]^\top$ and outputs $[\tilde{q}\ e\ u\ e]^\top$ with its state-space realization given by

$$\underline{P} \stackrel{s}{=} \left[\begin{array}{c|cccc} A_t & G & 0 & B & B \\ \hline H & 0 & 0 & 0 & 0 \\ -C & 0 & -I & 0 & 0 \\ 0 & 0 & 0 & 0 & I \\ -C & 0 & -I & 0 & 0 \end{array}\right]. \quad (19)$$

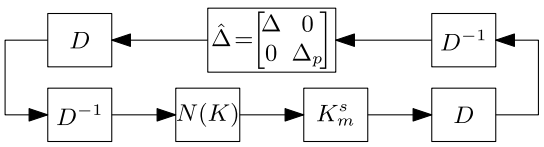

Fig. 8. Block diagram of the implementation for the skewed-μ DK-iteration procedure.

In this section, we have introduced an alternative robust performance framework. To design a controller that minimizes the skewed structured singular value $\mu_{\hat{\mathbf{\Delta}}}^s$, for the purpose of obtaining robust performance, a procedure to synthesize such controller, known as the DK-iteration procedure [40, Section 8.12], is treated concisely in Section IV-C.

C. Skewed-μ DK Iteration

This section focuses on the synthesis of a controller that minimizes a skewed structured singular value $\mu_{\hat{\mathbf{\Delta}}}^s$ to obtain closed-loop robust performance. The so-called skewed-μ DK-iteration procedure is used to synthesize a controller.

The first step in such DK-iteration procedure is the introduction of D-scaling matrices. This scaling uses the fact that $\hat{\Delta}$ is structured; hence, the inputs and outputs to $\hat{\Delta}$ and N are scaled by inserting the matrices D and D^{-1} as shown in Fig. 8. Using such scaling generally enables to find potentially tighter robust stability/performance conditions. For further details on the procedure, the reader is referred to [40] and [42].

The skewed-μ DK-iteration procedure aims at designing a controller that minimizes the peak value over frequency of the upper bound on the skewed structured singular value, i.e., a controller K should be designed by solving the following optimization problem:

$$\min_K \left(\min_D \| D K_m^s N(K) D^{-1} \|_\infty \right). \quad (20)$$

Here, the original scaling matrix $D(\omega)$ is replaced by a stable minimum-phase transfer function fit $D(s)$ of $D(\omega)$. The dependency of the closed-loop transfer function N on the controller K is indicated by $N(K)$. In DK iterations, a μ-analysis (D-step) and $\mathcal{H}_\infty$-optimization (K-step) are solved alternately (see [42]). In other words, the skewed-μ DK-iteration procedure alternates between minimizing (20) with respect to either K or D (while holding the other fixed) and recursively updating k_m^s (which characterizes K_m^s) during the D-step.

D. Closed-Loop Stability Analysis

The main purpose of the controller is to stabilize the equilibrium $\xi = 0$ of the nonlinear system (7). Let us assume

a controller K has been designed that meets the performance specifications and is robust with respect to the uncertainty Δ. Hence, the designed controller guarantees stability for the *linear* closed-loop system $N(s)$ and achieves robustness with respect to the uncertainty Δ. In this section, the stability of the *nonlinear* closed-loop system is considered. Therefore, we define a symmetric sector condition on the nonlinearity $\tilde{\varphi}$, such that for any (locally Lipschitz) nonlinearity that (locally) satisfies this sector condition, (local) asymptotic stability of the origin of the closed-loop system can be guaranteed.

We use the circle criterion [43, Th. 7.1] to determine a (symmetric) sector on the nonlinearity $\tilde{\varphi}$ for which robust stability can be guaranteed. Consider the closed-loop bit mobility (10) and a symmetric sector condition on the nonlinearity that is satisfied for all $\tilde{q} \in \mathcal{S}$ with $\mathcal{S} := \{\tilde{q} \in \mathbb{R} | \tilde{q}_l < \tilde{q} < \tilde{q}_u\}$ and $\tilde{q}_l < 0 < \tilde{q}_u$, i.e., $\tilde{\varphi}(\tilde{q}) \in [-\gamma, \gamma] \; \forall \; \tilde{q} \in \mathcal{S}$ and $\gamma > 0$. The nonlinear system is locally absolutely stable (i.e., $\xi = 0$ is locally asymptotically stable for any $\tilde{\varphi}(\tilde{q}) \in [-\gamma, \gamma]$ with $\tilde{q} \in \mathcal{S}$) if

$$H(s) = (1 + \gamma G_{\text{cl}}(s))(1 - \gamma G_{\text{cl}}(s))^{-1} \tag{21}$$

is strictly positive real. Applying [43, Lemma 6.1], a scalar transfer function $H(s)$ is strictly positive real if the following conditions are satisfied.

1) $H(s)$ is Hurwitz.
2) $\text{Re}[H(j\omega)] = \text{Re}[(1 + \gamma G_{\text{cl}}(j\omega)/1 - \gamma G_{\text{cl}}(j\omega))] > 0$, $\forall \omega \in \mathbb{R}$.
3) $H(\infty) > 0$.

For the symmetric sector, the condition on $H(s)$ being Hurwitz is equivalent to $G_{\text{cl}}(s)$ being Hurwitz. The closed-loop transfer function $G_{\text{cl}}(s)$ of the feedback interconnection is Hurwitz by the design of the stabilizing controller K. Moreover, G_{cl} is strictly proper, and therefore $H(\infty) = 1$, such that the third condition is satisfied. The second condition is equivalent to the condition

$$\|G_{\text{cl}}(j\omega)\|_\infty < \frac{1}{\gamma}. \tag{22}$$

Hence, the $\mathcal{H}_\infty$-norm of the closed-loop bit mobility G_{cl} gives an upper bound on the sector that the nonlinearity $\tilde{\varphi}$ should comply with, for the system to be absolutely stable. With the DK-iteration procedure, presented in Section IV-C, a controller K can be designed such that indeed $\|G_{\text{cl}}\|_\infty$ is minimized. In other words, the robustness with respect to uncertainty in the bit–rock interaction is optimized. This shows the benefit of employing the alternative robust performance technique (see Section IV-B) in terms of optimizing the robustness of the closed-loop drill-string dynamics with respect to the uncertainty in the bit–rock interaction, also in the nonlinear context.

In Section V, general design guidelines for the tuning of the weighting filters tailored to the drilling context are given and the designed controller is presented.

V. Controller Synthesis for Drilling Systems

Weighting filter design is key in satisfying the performance specifications related to, e.g., measurement noise sensitivity and actuator limitations as specified in the third controller objective, but also to ensure robustness with respect to the bit–rock interaction, through shaping of the bit mobility. To design a controller for a drill-string system, the following design guidelines should be taken into account for the weighting filters.

1) Include integral action to obtain the desired setpoint, i.e., in case of a mismatch between the (model-based) feedforward torque u_c and the actual required feedforward torque due to uncertainty in the model, integral action will compensate for this mismatch.
2) Include high-frequency roll-off to reduce measurement noise amplification.
3) Choose the cross-over frequency of the open-loop transfer function KG_{ol} (at the plant input) just above one of the dominant flexibility modes [e.g., the third eigenfrequency of the drill-string system (see Fig. 3)] to achieve damping of the dominant resonance modes.
4) Apply plant output scaling, i.e., scale the plant output $y = [\omega_{\text{td}} \; T_{\text{pipe}}]^\top$ such that the components of the weighted plant output $\bar{y}$ are in the same order of magnitude.

A. Weighting Filter Design

First, we apply plant scaling using the scaling matrices W_{sc} and V_{sc} [see Fig. 7]. This scaling is applied to compensate for the different orders of magnitude of the two plant outputs ω_{td} and T_{pipe}. The plant scaling matrices W_{sc} and V_{sc} are tuned to compensate for this effect and are given by

$$W_{\text{sc}} = \begin{bmatrix} w_{\text{sc1}} & 0 \\ 0 & w_{\text{sc2}} \end{bmatrix}, \quad V_{\text{sc}} = W_{\text{sc}}^{-1}$$

with $w_{\text{sc1}} = 10$ and $w_{\text{sc2}} = 0.01$.

The filters $V_1(s)$ and $W_1(s)$ can be used to shape the closed-loop bit mobility (G_{cl}). Ideally, the bit mobility should be damped as much as possible (as follows from the stability analysis in Section IV-D). However, this typically results in high control action. To deal with this tradeoff, the weighting filter $V_1(s)$ has two notch filters, to allow for a slightly less damped bit mobility at the locations of these filters, and is defined as follows:

$$V_1 = v_1 \frac{\frac{1}{(2\pi f_{1,1})^2}s^2 + \frac{2b_{1,1}}{2\pi f_{1,1}}s + 1}{\frac{1}{(2\pi f_{1,2})^2}s^2 + \frac{2b_{1,2}}{2\pi f_{1,2}}s + 1} \frac{\frac{1}{(2\pi f_{2,1})^2}s^2 + \frac{2b_{2,1}}{2\pi f_{2,1}}s + 1}{\frac{1}{(2\pi f_{2,2})^2}s^2 + \frac{2b_{2,2}}{2\pi f_{2,2}}s + 1}$$

with $f_{i,j}$ $(j = 1, 2)$ the frequencies of the notch filters and $b_{i,1}$ and $b_{i,2}$ $(i = 1, 2)$ parameters to tune the depth of the notch filter. The output weighting filter $W_1(s)$ is set to $W_1 = 1$, since tuning of $V_1(s)$ suffices to specify the desired bound on the closed-loop bit mobility.

The remaining weighting filters are designed to tune the closed-loop performance transfer functions. Let us first focus on the input weighting filters $V_2(s)$ and $V_3(s)$. The filter $V_2(s)$ is given by

$$V_2 = \begin{bmatrix} v_{21} & 0 \\ 0 & v_{22} \end{bmatrix}$$

with v_{21} and v_{22} static gains. Scaling of these gains allows for the synthesis of different controllers, i.e., differentiate between emphasis on specific controller objectives. The input weighting filter $V_3(s)$ is set as

$$V_3(s) = v_3 \|g_{\text{co}}\|^{-1} \frac{1}{w_{\text{sc1}}}$$

where v_3 is a static gain and $g_{\text{co}} := g_{22,1}(j2\pi f_{\text{co}})$, i.e., the subplant gain, related to input $\tilde{u}$ and output $\tilde{y}_1 = \omega_{\text{td}} - \omega_{\text{eq}}$, at the target cross-over frequency f_{co}. This gain is chosen to obtain a cross-over frequency of the open-loop transfer function KG_{ol} at 0.7 Hz. This cross-over frequency is chosen to achieve damping of the dominant resonance modes in the drill-string dynamics.

The output weighting filters $W_2(s)$ and $W_3(s)$ are also used to tune the closed-loop transfer functions, but, in addition, these filters are also used to apply the first two controller design guidelines, i.e., to include integral action and (first-order) roll-off. The (nonsquare) controller $K_t(s)$ to be designed has two inputs and a single output (due to the two measured signals of the plant), i.e., $K_t(s) = [K_{\omega_{\text{td}}}(s) \;\; K_{T_{\text{pipe}}}(s)]$. The controller aims at stabilizing the desired angular velocity setpoint. Note that due to the fact that K_t is nonsquare, a single integrator suffices to eliminate the steady-state error in both ω_{td} and T_{pipe}. Thus, the output weighting filter $W_2(s)$ is given by

$$W_2(s) = \begin{bmatrix} W_I(s) & 0 \\ 0 & w_{22} \end{bmatrix} = \begin{bmatrix} P_I \frac{s+2\pi f_I}{s} & 0 \\ 0 & w_{22} \end{bmatrix}$$

with $W_I(s)$ to obtain integral action in $K_{\omega_{\text{td}}}(s)$ and w_{22} a static gain. To obtain high-frequency roll-off, a roll-off filter is included in the output filter $W_3(s)$; hence

$$W_3(s) = w_3 w_{\text{sc1}} \|g_{\text{co}}\| W_R^{-1}$$

with w_3 a static gain and $W_R = (2\pi f_R/s + 2\pi f_R)$ the roll-off filter with roll-off frequency f_R.

The weighting filters $W_2(s)$ and $W_3(s)$ are unstable and nonproper weighting filters, respectively. Therefore, these filters are not applicable in the $\mathcal{H}_\infty$-controller synthesis. To circumvent this limitation and still obtain a controller that includes integral action and high-frequency roll-off, we use the method in [44].

The actual plant that is used in the controller synthesis algorithm is given by

$$G_t(s) = \text{diag}(1, \;\; W_I(s), \;\; 1) G_{\text{ol}}(s) \, \text{diag}(1, W_R(s)) \quad (23)$$

with $W_R(s)$ and $W_I(s)$ the roll-off and integrator filters, respectively. The resulting controller $K(s)$ from the DK-iteration procedure, treated in Section IV-C, for this plant G_t, has no integrator and roll-off properties. However, the actual controller for the plant G_{ol} can be calculated as follows:

$$K_t(s) = W_R(s) K(s) \, \text{diag}(W_I(s), \;\; 1) \quad (24)$$

which includes the desirable integrator and roll-off properties.

TABLE I

PARAMETER SETTINGS FOR THE PERFORMANCE WEIGHTING FILTERS THAT ARE EQUAL FOR THE DESIGNED HIGH-GAIN AND LOW-GAIN CONTROLLERS

Filter / setting	Parameters	
W_I	$f_I = 0.1$ Hz	$P_I = 0.1$
W_R	$f_R = 6$ Hz	
Cross-over frequency	$f_{\text{co}} = 0.7$ Hz	
V_1	$v_1 = 100$	
	$b_{1,1} = 0.15$	$b_{1,2} = 1.2$
	$f_{2,1} = 1.58$ Hz	$f_{2,2} = 1.58$ Hz
	$b_{2,1} = 0.05$	$b_{2,2} = 0.1$
V_2	$v_{21} = 5$	$v_{22} = 1.4$
V_3	$v_3 = 2$	
W_2	$w_{22} = 0.1$	

TABLE II

PARAMETER SETTINGS FOR THE PERFORMANCE WEIGHTING FILTERS THAT DIFFER FOR THE DESIGNED HIGH-GAIN AND LOW-GAIN CONTROLLERS

	Parameters	
Filter	High-gain controller	Low-gain controller
V_1	$f_{1,1} = 0.53$ Hz	$f_{1,1} = 0.48$ Hz
	$f_{1,2} = 0.35$ Hz	$f_{1,2} = 0.31$ Hz
W_3	$w_3 = \frac{1}{7}$	$w_3 = \frac{1}{3.1}$

B. Controller Synthesis Results

In this section, two controllers are synthesized based on the skewed-μ DK-iteration procedure and the proposed weighting filters from Section V-A. The two controllers mainly differ in the allowed control action and will be referred to as a *high-gain* (hg) controller and *low-gain* (lg) controller. The extra allowed control action for the high-gain controller is used to suppress the bit mobility even more compared with the low-gain controller. This distinction is made to illustrate the tradeoff between bit-mobility suppression, resulting in an increased operating envelope, and control action limitation, which is important from a practical point of view. In Table I, the parameters of the weighting filters that are equal for both controllers are summarized. The parameters that are changed for the two different controllers are given in Table II. The gain w_3 is used to allow for less (or more) control action and the notch filter in $V_1(s)$ is used to allow for a higher bit mobility in specific frequency ranges.

Performing the DK-iteration procedure for the drill-string system with the weighting filters as specified above results in controllers $K_t(s) = [K_{\omega_{\text{td}}}(s), \;\; K_{T_{\text{pipe}}}(s)]$, as shown in Fig. 9 for both the high-gain and the low-gain controllers. From Fig. 9, the integral action in the controller, $K_{\omega_{\text{td}}}(s)$, that uses the top drive angular velocity can be clearly recognized. Moreover, the first-order roll-off is present in both controllers. It can also be seen that the designed controllers are active in the frequency range of the torsional resonance modes of the drill-string system (see Fig. 3), which is not the case for the state-of-practice SoftTorque controller shown in Fig. 9. This industrial controller, which uses only top drive velocity

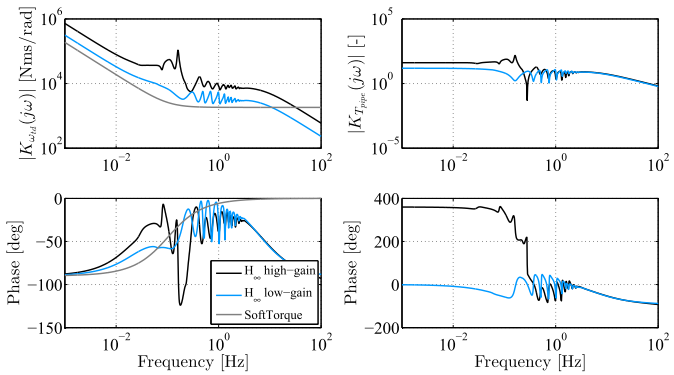

Fig. 9. Designed linear dynamic controllers for the drill-string system. Left: the controller that uses the top drive angular velocity measurement. Right: the controller is based on the pipe torque measurement.

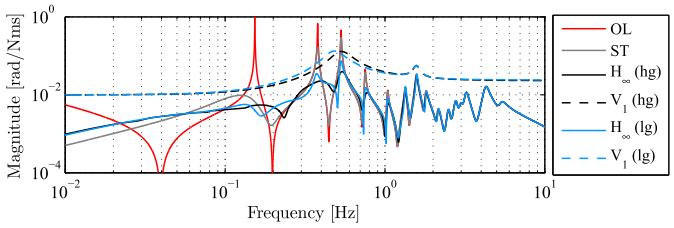

Fig. 10. Closed-loop bit mobility, i.e., the frequency response function from bit torque T_{bit} to bit velocity ω_{bit}. The bit mobility of system with the high-gain (hg) and low-gain (lg) controller is shown and compared with the open-loop (OL) bit mobility and the bit mobility induced by the industrial controller (ST). Moreover, the weighting filter V_1 to tune the bit mobility for the high-gain and low-gain controllers is shown. It can be seen that both the high-gain and low-gain controllers suppress the bit mobility significantly.

measurements, is a properly tuned active damping system (i.e., PI control of the angular velocity), which aims at damping the first torsional mode of the drill-string dynamics. A comparison with this controller by means of a simulation is presented in Section VI.

The closed-loop bit mobility for the different controllers is shown in Fig. 10 and also compared with the open-loop (OL) bit mobility and the bit mobility induced by the industrial controller [SoftTorque (ST)]. Moreover, the bounds, specified by the weighting filter V_1, for the controller synthesis are indicated by the dashed lines. It can be seen that the high-gain controller suppresses the bit mobility the most, but also with the low-gain controller, a significant decrease in the peak value of the bit mobility is achieved compared with the industrial controller. Let us now determine the $\mathcal{H}_\infty$-norm for the closed-loop system $G_{\text{cl}}^{\text{hg}}(s)$ with the high-gain controller

$$\left\| G_{\text{cl}}^{\text{hg}}(s) \right\|_\infty = \sup_\omega \left| G_{\text{cl}}^{\text{hg}}(j\omega) \right| = 0.039. \tag{25}$$

For comparison, for the low-gain controller, the $\mathcal{H}_\infty$-norm is equal to $\|G_{\text{cl}}^{\text{lg}}(s)\|_\infty = 0.074$ and for the industrial controller $\|G_{\text{cl}}^{\text{ST}}(s)\|_\infty = 0.298$. Hence, with the high-gain controller, the peak value of the bit mobility has been decreased with almost a factor of eight. It can also be seen in Fig. 10 that multiple modes of the bit mobility are damped by the controllers obtained with the proposed controller design strategy, while with the SoftTorque controller only significant damping of the first torsional mode is achieved.

According to (22), the sector (for $\tilde{\varphi}$) for which stability can now be guaranteed is equal to $[-\gamma_{\text{hg}}, \gamma_{\text{hg}}]$ with

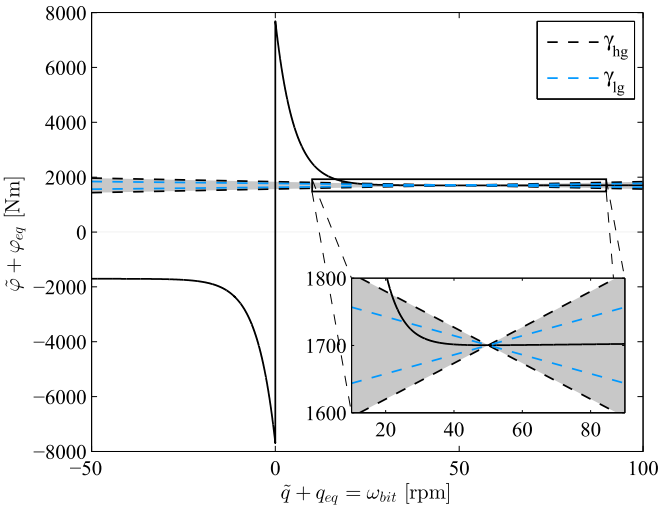

Fig. 11. Transformed bit–rock interaction model $\tilde{\varphi}(\tilde{q})$ and maximal sector condition for the high-gain and low-gain controllers.

$\gamma_{\text{hg}} = 1/0.039 = 25.46$ (for the high-gain controller). In Fig. 11, the nonlinearity $\tilde{\varphi}+\varphi_{\text{eq}}$ is shown, including the sector $[-\gamma_{\text{hg}}, \gamma_{\text{hg}}]$ (and $[-\gamma_{\text{lg}}, \gamma_{\text{lg}}]$ for reference). From Fig. 11, it can be seen that the closed-loop nonlinear system is locally absolutely stable, as long as the bit angular velocity is larger than (approximately) 22 r/min (because $\tilde{q} + Hx_{\text{eq}} = \omega_{\text{bit}}$). To conclude, with the designed controllers, robustness with respect to uncertainty in the bit–rock interaction is achieved for a substantial variation in the bit velocity. This is a key aspect of the designed controllers since it directly relates to the first two controller objectives (see Section II-B).

VI. Simulation Results

Simulation results of the controllers designed in Section V, applied to the nonlinear drill-string model presented in Section III, are presented in Section VI-C. First in Section VI-A, we introduce the startup scenario, which is used for the simulation studies. In Section VI-B, we present a simulation result of the drill-string system in closed-loop with an existing industrial controller (based on [5]) as a state-of-practice reference case.

A. Startup Scenario

For the simulations, we introduce a so-called startup scenario, which is based on practical startup procedures for drilling rigs. Herein, the drill string is first accelerated to a low constant rotational velocity, starting from zero angular velocity for the whole drill string, with the bit above the formation (off bottom). Subsequently, the angular velocity and WOB are gradually increased to the desired operating conditions. The increase in WOB is modeled as a scaling of the bit–rock interaction torque. Assume that the WOB is scaled according to the following profile:

$$\alpha(t) = \begin{cases} 0, & t_0 \le t \le t_1 \\ \frac{t-t_1}{t_2-t_1}, & t_1 < t < t_2 \\ 1, & t \ge t_2 \end{cases} \tag{26}$$

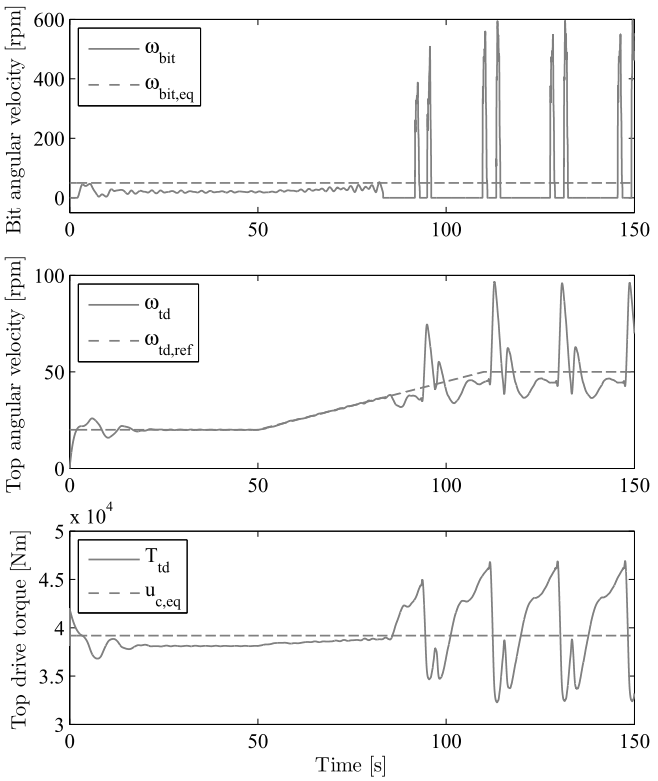

Fig. 12. Simulation result of the drill-string model with an existing industrial (SoftTorque) controller in the startup scenario, which clearly shows stick-slip vibrations in the bit angular velocity (top).

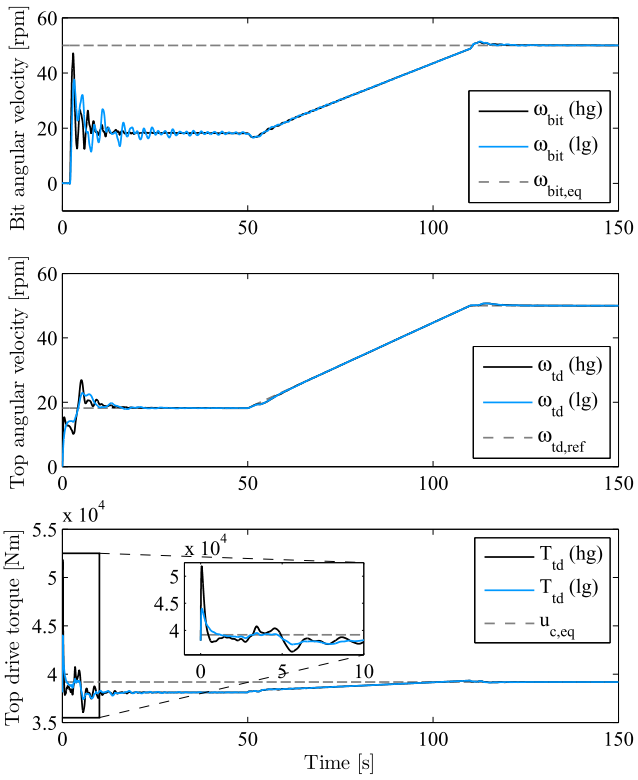

Fig. 13. Simulation result of the drill-string model with the designed output-feedback controllers in the startup scenario. Both the top drive and bit angular velocity converge to their setpoint and stick-slip vibrations are avoided.

where $\alpha = 0$ means bit off bottom and $\alpha = 1$ indicates full WOB and with $t_1 = 50$ s and $t_2 = 110$ s in this case. Then the bit–rock interaction model is scaled using this scaling factor $\alpha(t)$; hence

$$T_{\text{bit}}(t) = \text{Sign}(\omega_{\text{bit}})(T_{\text{ini}} + \alpha(t)(T_d - T_{\text{ini}} + (T_s - T_d)e^{-\frac{30}{N_d\pi}|\omega_{\text{bit}}|})) \quad (27)$$

where T_{ini} is the amount of resisting torque that is still present, even when the bit is off bottom (e.g., due to drilling mud and interactions with the borehole). Note that for WOB $= 0$ (off bottom), there is no velocity weakening in the TOB. The startup scenario comprises the following steps.

1) Start with WOB $= 0$ and operate at relatively low velocity (starting from initial zero velocity for the whole drill string) to build up torque in drill string to overcome static torques due to drag in the time window $0 < t < 50 = t_1$ s.
2) Slowly increase the reference angular velocity until the desired operating velocity (ω_{eq}) is reached (in the time window $t_1 = 50 \leq t < 110 = t_2$ s). At the same time, slowly increase the WOB and finally obtain the nominal operating condition in the angular velocity and WOB.

This startup scenario is used for all simulations in Sections VI.A–VI.C and VII.A–VII.C. Summarizing, the initial conditions for the drill string are an undeformed stationary drill string (i.e., zero angular velocities and displacements) and no top drive torque applied.

B. Simulation Result of the Industrial Controller

A simulation result of the drill-string model (5) in feedback with the industrial controller (as shown in Fig. 9) is shown in Fig. 12. The top drive velocity (ω_{td}) is shown along with the reference velocity $\omega_{\text{td,ref}}$ that starts at a velocity of 20 r/min and is gradually increased to the desired equilibrium velocity, ω_{eq}, of 50 r/min. From the bit response, in Fig. 12 (top), we can clearly recognize stick-slip oscillations. The increasing amplitude of the oscillations in the top drive velocity and top drive torque (bottom plot) demonstrates that these vibrations arise when the WOB is increased ($50 \leq t < 110$ s), i.e., when due to scaling of the TOB the velocity weakening in the bit–rock interaction effect starts affecting the dynamics. Stick-slip oscillations arise as a consequence of the fact that this industrial controller does not attenuate higher flexibility modes in the bit mobility (see Fig. 10), as is evidenced by the frequency content of the transient oscillations in the bit velocity before stick occurs [see Fig. 12 (top)].

C. Simulation Results of the Designed Controllers

Simulation results of the designed controllers in Fig. 9 are shown in Fig. 13. The same startup scenario and initial conditions, as in Fig. 12, are used for these simulations. The simulation results show that the top drive and bit angular velocity converge to their setpoint and stick-slip vibrations are avoided. The controllers are able to stabilize the desired setpoint, because damping of multiple flexibility modes is

achieved and robustness with respect to the bit–rock interaction is taken into account in the design. The difference between the low gain and the high gain is particularly visible in the top drive torque; the high-gain controller acts more aggressively in response to the initial error, resulting in more control action (see the zoomed-in plot). Consequently, this results in transient oscillations with a larger amplitude in the angular velocity of the drill string, as can be seen in both the top drive velocity and the bit velocity. On the other hand, the amplitude of the oscillations decays faster for the high-gain controller compared with the low-gain controller, in particular at the bit, which is a result of increased bit-mobility suppression obtained by the high-gain controller.

The simulation results in this section are performed under nominal conditions. In Section VII, robustness with respect to different operating velocities, changing bit–rock interaction, and increased drill-string length is investigated.

VII. Robustness of the Closed-Loop System

As already stated in the controller objectives in Section II-B, robustness of the closed-loop system is an important objective of the proposed controller design strategy. Several key aspects regarding the robustness of the closed-loop drill-string system are investigated in this section. In Section VII-A, robustness with respect to different operating velocities is investigated. In Section VII-B, robustness with respect to uncertainty in the bit–rock interaction is investigated, and in Section VII-C, the influence of the increasing length of the drill string while drilling is examined. Although not specifically treated in this paper, it can also be shown that the proposed controller can effectively deal with sensor and actuator noise due to the roll-off filter that is incorporated in the controller (see [39]). Moreover, preliminary experimental results are presented in [39], where the controller design strategy is applied on a low-order (i.e., 4-DOF) drill-string setup. The experimental results indicate the potential of the controllers developed in this paper.

A. Different Operating Velocities

In practice, the desired operating conditions, in terms of the desired angular velocity, may change. To avoid time consuming retuning of the controller when the desired velocity is changed, the controller should be applicable for a wide range of desired operating velocities.

Due to the velocity-weakening effect in the nonlinear bit–rock interaction, lower angular velocities are more difficult to stabilize compared with higher angular velocities. Therefore, the applicability of the high-gain controller at lower angular velocities is investigated. A simulation with the startup scenario and a desired angular velocity of 35 r/min has been performed and the result is shown in Fig. 14. The first 50 s are equal to the simulation results shown in Fig. 13 as the initial conditions and starting velocity (20 r/min) are the same. Clearly, the controller is able to stabilize the desired setpoint of 35 r/min (under the imposed operating conditions). This shows that a significant increase in the operating envelope in terms of angular velocity can be achieved as the industrial controller is not even able to stabilize the significantly higher desired angular velocity of 50 r/min (see Section VI-B).

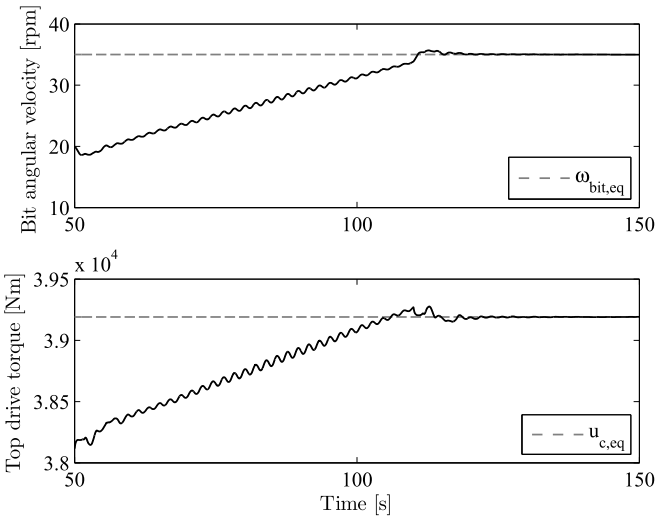

Fig. 14. Simulation result of the drill-string model in the startup scenario with the high-gain controller and a desired angular velocity of 35 r/min.

B. Changing Bit–Rock Interaction Model

Robustness with respect to uncertainty in the bit–rock interaction is an important property of the closed-loop system from a practical point of view, first of all because it is difficult to obtain an accurate model of the bit–rock interaction. Another reason is the fact that the bit–rock interaction is prone to changes during the drilling process, for example, due to bit wear and changes in the rock formation. Therefore, one of the controller objectives (Section II-B) is to obtain robustness with respect to uncertainty in the bit–rock interaction. In Fig. 11, the sector condition on the bit–rock interaction has already been visualized. This sector conditions state that the desired equilibrium point is (locally) absolutely stable for any bit–rock interaction within the sector, i.e., the gray area in Fig. 11 for the high-gain controller. In this section, we present a simulation result of the drill-string system in closed loop with the designed high-gain controller to illustrate the robustness with respect to changes in the bit–rock interaction.

Recall the nominal parameter values for the bit–rock interaction model, that is, $T_s = 7700$ Nm, $T_d = 1700$ Nm, and $N_d = 5$ r/min, which are used for the controller synthesis. In this simulation study, both the torque level and the decrease rate of the bit–rock interaction are changed. The parameters for the adapted bit–rock interaction model are given by $T_s^c = T_s + 200$, $T_d^c = T_d + 200$, and $N_d^c = N_d + 1$. The adapted bit–rock interaction model is shown in Fig. 15; the adapted model has a less severe velocity-weakening effect at low velocities and therefore more negative damping at higher velocities. The value of N_d is chosen such that the bit–rock interaction still locally satisfies the sector condition. The simulation is started with the same settings as the simulation results shown before. However, to test robustness, at $t = 130$ s, the bit–rock interaction model is suddenly

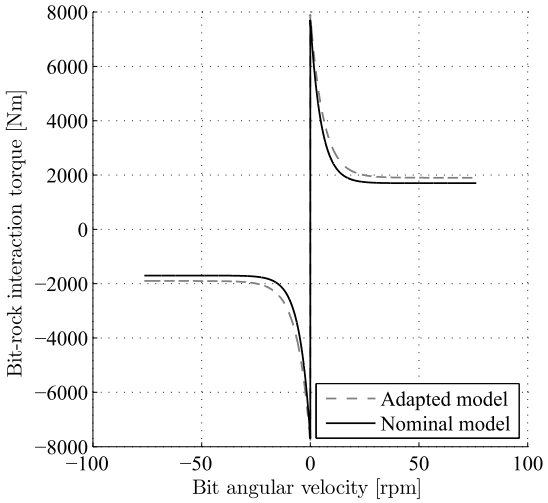

Fig. 15. Nominal and adapted bit–rock interaction model.

changed to the adapted parameter settings. The TOB changes instantaneously from approximately 1700 to approximately 1900 Nm as shown in the second plot in Fig. 16. Due to oscillations in the bit angular velocity, it peaks further up to approximately 1950 Nm. This change is relatively large compared with the allowed variation in the bit–rock interaction for which the sector condition holds (see Fig. 11 for the nominal bit–rock interaction). As can be seen from the other plots, the change in bit–rock interaction causes some oscillations in the states of the drill-string system. Still, the oscillations are damped and the velocities of both the top drive and the bit converge to the desired angular velocity. In the zoomed-in plot of the top drive torque, it can be seen that the top drive torque converges to a new equilibrium value that is slightly higher than the original equilibrium. A closer study of the new equilibrium value shows that it exactly compensates for the added 200 Nm in torque of the adapted bit–rock interaction model. This illustrates the effect of the integral action in the controller; due to the integral action in the top drive velocity part ($K_{\omega_{\text{td}}}$) of the controller, the desired velocity is stabilized, resulting in a new equilibrium value for the top drive torque.

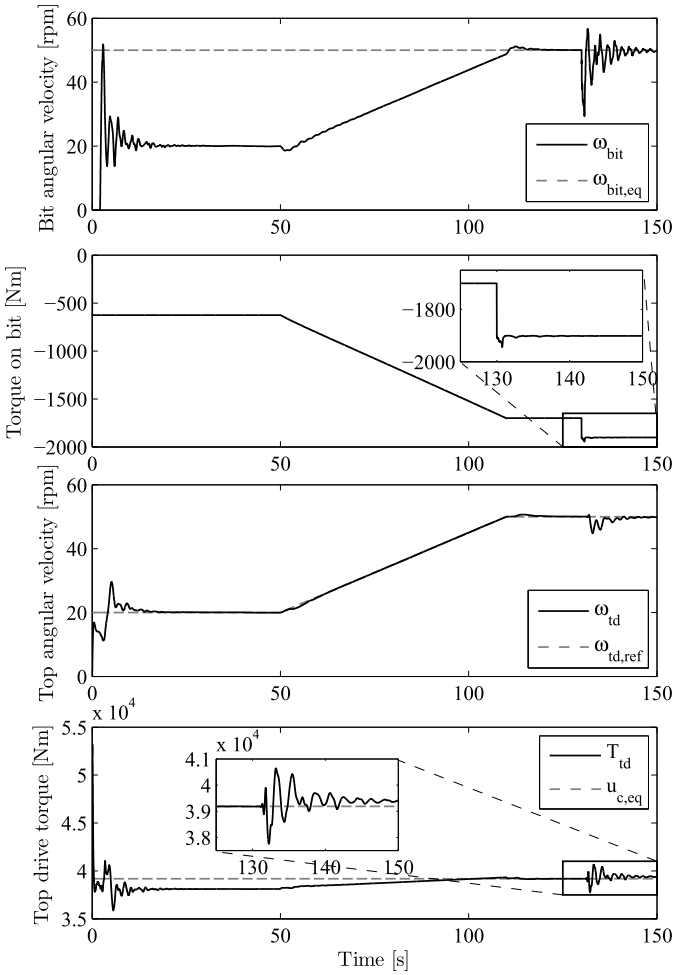

Fig. 16. Simulation result of the drill-string model in the startup scenario with the high-gain controller and a change in the bit–rock interaction at $t = 130$ s. The oscillations caused by the change in the bit–rock interaction are damped and the angular velocities converge to the desired angular velocity.

C. Changing Length of the Drill String

During the drilling process, the drill string is gradually lengthened as the well becomes deeper. Current controllers need to be retuned during the drilling operation and this retuning is prone to errors, resulting in wrong controller settings and possibly failing of the stick-slip mitigation due to tuning errors. Additionally, the retuning process is time consuming, and therefore the amount of tuning occurrences should be minimized. In other words, the controller should be robust with respect to the increasing length of the drill string. In this section, the plant model (5) is changed such that the dynamics of the plant correspond to a drill-string of different length.

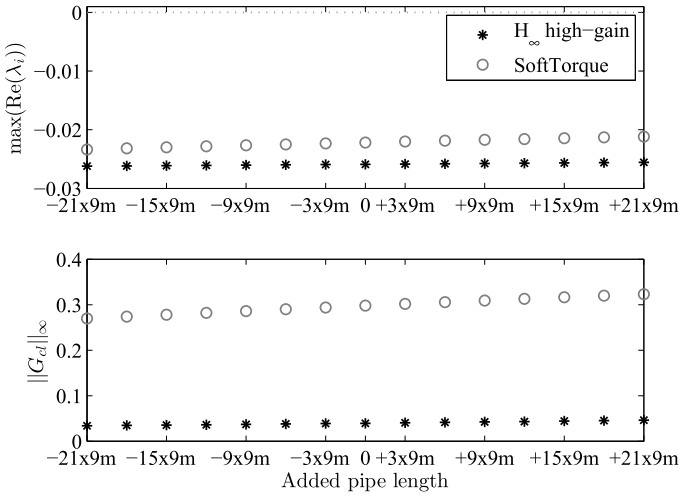

Fig. 17. Location of the right-most pole of the closed-loop system (top) and $\mathcal{H}_\infty$-norm of the bit mobility (bottom) as a function of added pipe length to the drill string.

In practice, to add a new pipe section, the drill string is stopped and a stand of one or multiple drill pipes is connected to the drill string. Here, it is assumed that a new stand of three drill pipes is added to the drill string (i.e., 27 m of length is added to the drill string). In practical situations, the current industrial controller needs to be retuned every stand, and

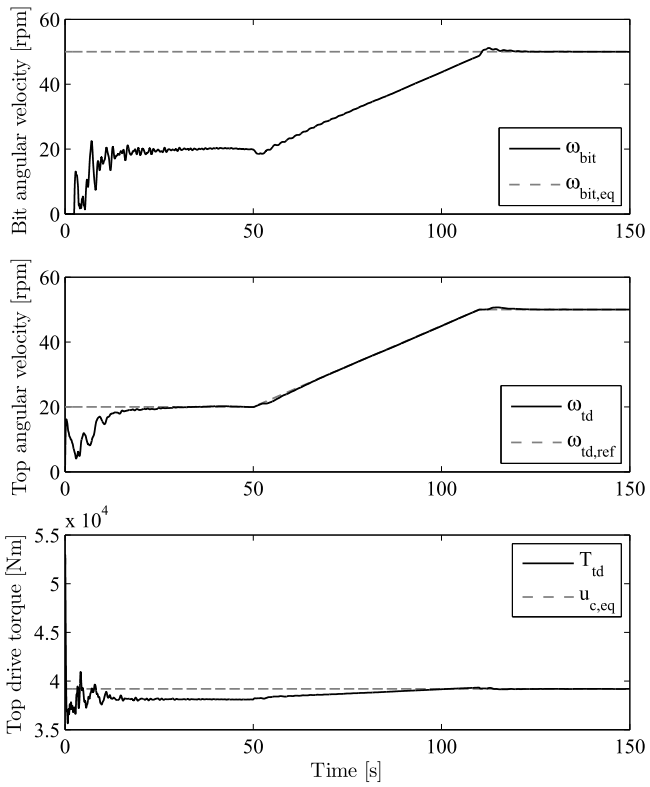

Fig. 18. Simulation result of the drill-string model in the startup scenario with the high-gain controller and a drill-string model with increased length (21×9 m^2 added drill pipe).

sometimes even after one or two added drill pipes. The pole locations of the closed-loop system, consisting of a changed plant model and a controller designed for the nominal drill string, are investigated for different controllers. The results of the analysis of the high-gain $\mathcal{H}_\infty$-controller are shown in Fig. 17 and compared with the industrial controller. The real value of the right-most pole is shown as a function of changing length compared with the nominal model. The right-most pole of the nominal model (indicated by 0) lies in the left-half-plane (LHP) for both controllers. When the length of the drill string is decreased, the right-most pole moves further into the LHP, while for an increase in length, the right-most pole moves toward the imaginary axis.

As mentioned before, the location of the eigenvalue is not the only important factor, as local asymptotic stability does not imply that no stick-slip vibrations occur. Clearly, SoftTorque also locally asymptotically stabilizes the system, but stick-slip oscillations still occur. Therefore, the $\mathcal{H}_\infty$-norm of the bit mobility (G_{cl}) is also shown. The $\mathcal{H}_\infty$-norm of the closed-loop bit mobility with the high-gain $\mathcal{H}_\infty$-controller is approximately a factor 7 lower than the $\mathcal{H}_\infty$-norm of G_{cl} with the industrial controller (also see Fig. 10 for the nominal case). This indicates that the $\mathcal{H}_\infty$-controller has significantly more robustness with respect to bit–rock interaction variations than the industrial controller and is therefore able to stabilize the desired setpoint (and avoid stick-slip vibrations) as shown in the previous simulations, while the industrial controller is unable to do so.

Changing the length of the drill-string does not have a large effect on the pole locations and $\mathcal{H}_\infty$-norm as can be seen in Fig. 17. However, it has to be noted that when 15 or more pipe sections are added to the drill string, the system controlled with the low-gain controller has an unstable equilibrium point. For the high-gain controller, the right-most pole is still in the LHP and the $\mathcal{H}_\infty$-norm is only slightly increased when the length of the drill string is increased. A simulation result of a plant model that is 189 m (21×9 m) longer than the nominal model (which has a total length of 6249 m) and controlled with the high-gain $\mathcal{H}_\infty$-controller is shown in Fig. 18. This simulation confirms that the desired equilibrium is indeed stable with this controller. This means that this controller is able to stabilize the desired setpoint of drill-string systems for a large variation in length of the drill string. It can be concluded that a significant increase in robustness with respect to increasing drill-string length is obtained compared with the industrial controller.

VIII. Conclusion

In this paper, a novel synthesis strategy for controllers aiming at the mitigation of torsional stick-slip oscillations in drilling systems is developed. The controller design is based on skewed-μ DK iteration and offers several benefits over pre-existing controllers. First, the designed controller is applicable to a multimodal drill-string model while guaranteeing (local) stability of the desired operating point. Second, the controller is optimized to have robustness with respect to uncertainty in the bit–rock interaction. Third, performance specifications regarding measurement noise sensitivity and actuator limitation are integrated in the controller design. Fourth, the controller uses only surface measurements, which is a key requirement from practical point of view. Simulation results of the proposed controller applied to the 18-DOF drill-string model show that the stick-slip oscillations are eliminated in realistic drilling scenarios in which an existing industrial controller shows stick-slip vibrations.

From a practical point of view, several robustness aspects have been investigated. It has been shown that a significant increase in the operating envelope of the drill-string system is achieved, both in terms of angular velocity and increasing length of the drill string. Another aspect that is investigated is robustness with respect to uncertainty in the bit–rock interaction. Simulation results have shown that a sudden change in the bit–rock interaction can be effectively dealt with by the proposed controller.

Summarizing, it is concluded that the proposed controller can effectively deal with practical drilling conditions and it outperforms currently used industrial controllers in terms of the operating envelope for which stick-slip oscillations can be eliminated.

Appendix
System Matrices

The system matrices of the model given in (1) are given in the following:

$$M = \begin{bmatrix} 1.6996 & 0.8498 & 0 & \cdots & \cdots & \cdots & \cdots & \cdots & \cdots & \cdots & \cdots & 0 \\ 0.8498 & 5.4902 & 1.895 & 0 & & & & & & & & \vdots \\ 0 & 1.8953 & 4.7717 & 0.4906 & 0 & & & & & & & \vdots \\ \vdots & 0 & 0.4906 & 4.7030 & 1.8609 & 0 & & & & & & \vdots \\ \vdots & & 0 & 1.8609 & 7.4436 & 1.8609 & 0 & & & & & \vdots \\ \vdots & & & 0 & 1.8609 & 7.4436 & 1.8609 & 0 & & & & \vdots \\ \vdots & & & & 0 & 1.8609 & 7.4436 & 1.8609 & 0 & & & \vdots \\ \vdots & & & & & 0 & 1.8609 & 32.420 & 14.349 & 0 & & \vdots \\ \vdots & & & & & & 0 & 14.349 & 57.396 & 14.349 & \ddots & \vdots \\ \vdots & & & & & & & \ddots & \ddots & \ddots & \ddots & 0 \\ \vdots & & & & & & & & 0 & 14.349 & 57.396 & 14.349 \\ 0 & \cdots & \cdots & \cdots & \cdots & \cdots & \cdots & \cdots & \cdots & 0 & 14.349 & 1806.7 \end{bmatrix} \tag{28}$$

$$D = \begin{bmatrix} 155.44 & -155.44 & 0 & \cdots & \cdots & \cdots & \cdots & \cdots & \cdots & \cdots & \cdots & 0 \\ -155.44 & 162.92 & -7.4797 & 0 & & & & & & & & \vdots \\ 0 & -7.4797 & 275.38 & -267.90 & 0 & & & & & & & \vdots \\ \vdots & 0 & -267.90 & 272.16 & -4.2668 & 0 & & & & & & \vdots \\ \vdots & & 0 & -4.2668 & 8.5337 & -4.2668 & 0 & & & & & \vdots \\ \vdots & & & 0 & -4.2668 & 8.5337 & -4.2668 & 0 & & & & \vdots \\ \vdots & & & & 0 & -4.2668 & 8.5337 & -4.2668 & 0 & & & \vdots \\ \vdots & & & & & 0 & -4.2668 & 12.988 & -8.7212 & 0 & & \vdots \\ \vdots & & & & & & 0 & -8.7212 & 17.443 & -8.7212 & \ddots & \vdots \\ \vdots & & & & & & & \ddots & \ddots & \ddots & \ddots & 0 \\ \vdots & & & & & & & & 0 & -8.7212 & 17.443 & -8.7212 \\ 0 & \cdots & \cdots & \cdots & \cdots & \cdots & \cdots & \cdots & \cdots & 0 & -8.7212 & 8.7212 \end{bmatrix} \tag{29}$$

$$K_t = \begin{bmatrix} 4.8833 & 0 & \cdots & \cdots & \cdots & \cdots & \cdots & \cdots & \cdots & \cdots & 0 \\ -4.8833 & 0.2350 & 0 & & & & & & & & \vdots \\ 0 & -0.2350 & 8.4162 & 0 & & & & & & & \vdots \\ \vdots & 0 & -8.4162 & 0.1340 & 0 & & & & & & \vdots \\ \vdots & & 0 & -0.1340 & 0.1340 & 0 & & & & & \vdots \\ \vdots & & & 0 & -0.1340 & 0.1340 & 0 & & & & \vdots \\ \vdots & & & & 0 & -0.1340 & 0.1340 & 0 & & & \vdots \\ \vdots & & & & & 0 & -0.1340 & 0.1340 & 0 & & \vdots \\ \vdots & & & & & & 0 & -0.1340 & 0.2740 & 0 & \vdots \\ \vdots & & & & & & & 0 & -0.2740 & 0.2740 & \ddots & \vdots \\ \vdots & & & & & & & & \ddots & \ddots & \ddots & 0 \\ \vdots & & & & & & & & & 0 & -0.2740 & 0.2740 \\ 0 & \cdots & \cdots & \cdots & \cdots & \cdots & \cdots & \cdots & \cdots & 0 & -0.2740 & \end{bmatrix} \cdot 10^4 \tag{30}$$

$$S_w = \begin{bmatrix} 0 & \cdots & \cdots & 0 \\ 1 & \ddots & & \vdots \\ 0 & \ddots & \ddots & \vdots \\ \vdots & \ddots & \ddots & 0 \\ 0 & \cdots & 0 & 1 \end{bmatrix}, \quad S_b = \begin{bmatrix} 1 \\ 0 \\ \vdots \\ 0 \end{bmatrix}, \quad S_t = \begin{bmatrix} 0 \\ \vdots \\ 0 \\ 1 \end{bmatrix} \tag{31}$$

REFERENCES

[1] N. Challamel, "Rock destruction effect on the stability of a drilling structure," *J. Sound Vibrat.*, vol. 233, no. 2, pp. 235–254, 2000.

[2] A. P. Christoforou and A. S. Yigit, "Fully coupled vibrations of actively controlled drillstrings," *J. Sound Vibrat.*, vol. 267, no. 5, pp. 1029–1045, 2003.

[3] J. D. Jansen, "Nonlinear dynamics of oilwell drillstrings," Ph.D. dissertation, Dept. Mech. Maritime Mater. Eng., Delft Univ. Technol., Delft, The Netherlands, 1993.

[4] Y. A. Khulief, F. A. Al-Sulaiman, and S. Bashmal, "Vibration analysis of drillstrings with self-excited stick–slip oscillations," *J. Sound Vibrat.*, vol. 299, no. 3, pp. 540–558, 2007.

[5] J. D. Jansen and L. van den Steen, "Active damping of self-excited torsional vibrations in oil well drillstrings," *J. Sound Vibrat.*, vol. 179, no. 4, pp. 647–668, 1995.

[6] A. F. A. Serrarens, M. J. G. van de Molengraft, J. J. Kok, and L. van den Steen, "H_∞ control for suppressing stick-slip in oil well drillstrings," *IEEE Control Syst.*, vol. 18, no. 2, pp. 19–30, Apr. 1998.

[7] J. C. A. de Bruin, A. Doris, N. van de Wouw, W. P. M. H. Heemels, and H. Nijmeijer, "Control of mechanical motion systems with non-collocation of actuation and friction: A Popov criterion approach for input-to-state stability and set-valued nonlinearities," *Automatica*, vol. 45, no. 2, pp. 405–415, 2009.

[8] T. Richard, C. Germay, and E. Detournay, "A simplified model to explore the root cause of stick–slip vibrations in drilling systems with drag bits," *J. Sound Vibrat.*, vol. 305, no. 3, pp. 432–456, 2007.

[9] C. Germay, N. Van de Wouw, H. Nijmeijer, and R. Sepulchre, "Nonlinear drillstring dynamics analysis," *SIAM J. Appl. Dyn. Syst.*, vol. 8, no. 2, pp. 527–553, 2009.

[10] K. Nandakumar and M. Wiercigroch, "Stability analysis of a state dependent delayed, coupled two DOF model of drill-stringvibration," *J. Sound Vibrat.*, vol. 332, no. 10, pp. 2575–2592, 2013.

[11] C. Germay, V. Denoël, and E. Detournay, "Multiple mode analysis of the self-excited vibrations of rotary drilling systems," *J. Sound Vibrat.*, vol. 325, nos. 1–2, pp. 362–381, 2009.

[12] B. Besselink, T. Vromen, N. Kremers, and N. van de Wouw, "Analysis and control of stick-slip oscillations in drilling systems," *IEEE Trans. Control Syst. Technol.*, vol. 24, no. 5, pp. 1582–1593, Sep. 2016.

[13] P. D. Spanos, A. M. Chevallier, N. P. Politis, and M. L. Payne, "Oil well drilling: A vibrations perspective," *Shock Vibrat. Dig.*, vol. 35, no. 2, pp. 81–99, 2003.

[14] M. Karkoub, M. Zribi, L. Elchaar, and L. Lamont, "Robust μ-synthesis controllers for suppressing stick-slip induced vibrations in oil well drill strings," *Multibody Syst. Dyn.*, vol. 23, no. 2, pp. 191–207, 2010.

[15] G. W. Halsey, A. Kyllingstad, and A. Kyllingstad, "Torque feedback used to cure slip-stick motion," in *Proc. SPE Annu. Tech. Conf. Exhib.*, Houston, TX, USA, Oct. 1988, pp. 277–282.

[16] T. Ritto, "Numerical analysis of the nonlinear dynamics of a drill-string with uncertainty modeling," Ph.D. dissertation, Univ. Paris-Est, Champs-sur-Marne, France, 2010.

[17] A. Cunha, Jr., C. Soize, and R. Sampaio, "Exploring the nonlinear dynamics of horizontal drillstrings subjected to friction and shocks effects," in *Proc. 21th Congr. Numer. Methods Appl., MeCom (ENIEF)*, Bariloche, Argentina, Sep. 2014, pp. 1–11.

[18] P. J. Nessjøen, A. Kyllingstad, P. D'Ambrosio, I. S. Fonseca, A. Garcia, and B. Levy, "Field experience with an active stick-slip prevention system," in *Proc. SPE/IADC Drilling Conf. Exhib.*, Amsterdam, The Netherlands, Mar. 2011, pp. 139956-1–139956-10.

[19] D. J. Runia, S. Dwars, and I. P. J. M. Stulemeijer, "A brief history of the shell 'soft torque rotary system' and some recent case studies," in *Proc. 2nd Int. Colloq. Nonlinear Dyn. Control Deep Drilling Syst.*, Eindhoven, The Netherlands, May 2012, pp. 69–76.

[20] E. Fridman, S. Mondié, and B. Saldivar, "Bounds on the response of a drilling pipe model," *IMA J. Math. Control Inf.*, vol. 27, no. 4, pp. 513–526, 2010.

[21] A. G. Balanov, N. B. Janson, P. V. E. McClintock, R. W. Tucker, and C. H. T. Wang, "Bifurcation analysis of a neutral delay differential equation modelling the torsional motion of a driven drill-string," *Chaos, Solitons, Fractals*, vol. 15, no. 2, pp. 381–394, 2003.

[22] I. Boussaada, H. Mounier, S.-I. Niculescu, and A. Cela, "Analysis of drilling vibrations: A time-delay system approach," in *Proc. 20th Meditteranean Conf. Control Autom.*, Barcelona, Spain, Jul. 2012, pp. 610–614.

[23] D. Bresch-Pietri and M. Krstic, "Adaptive output-feedback for wave PDE with anti-damping—Application to surface-based control of oil drilling stick-slip instability," in *Proc. 53rd IEEE Conf. Decision Control*, Los Angeles, CA, USA, Dec. 2014, pp. 1295–1300.

[24] B. Saldivar, S. Mondié, J.-J. Loiseau, and V. Rasvan, "Suppressing axial-torsional coupled vibrations in drillstrings," *J. Control Eng. Appl. Inform.*, vol. 15, no. 1, pp. 3–10, 2013.

[25] W. R. Tucker and C. Wang, "On the effective control of torsional vibrations in drilling systems," *J. Sound Vibrat.*, vol. 224, no. 1, pp. 101–122, 1999.

[26] E. Kreuzer and M. Steidl, "Controlling torsional vibrations of drill strings via decomposition of traveling waves," *Arch. Appl. Mech.*, vol. 82, no. 4, pp. 515–531, 2012. [Online]. Available: http://dx.doi.org/10.1007/s00419-011-0570-8

[27] V. Denoël and E. Detournay, "Eulerian formulation of constrained elastica," *Int. J. Solids Struct.*, vol. 48, nos. 3–4, pp. 625–636, 2011.

[28] A. Doris, "Method and system for controlling vibrations in a drilling system," WO Patent 2013 076184 A3, Mar. 27, 2014.

[29] T. Vromen, N. van de Wouw, A. Doris, P. Astrid, and H. Nijmeijer, "Nonlinear output-feedback control of torsional vibrations in drilling systems," *Int. J. Robust Nonlinear Control*, 2017, doi: 10.1002/rnc.3759.

[30] F. Abdulgalil and H. Siguerdidjane, "Nonlinear control design for suppressing stick-slip oscillations in oil well drillstrings," in *Proc. 5th Asian Control Conf.*, vol. 2. Jul. 2004, pp. 1276–1281.

[31] S. Dwars, "Recent advances in soft torque rotary systems," in *Proc. SPE/IADC Drilling Conf. Exhib.*, London, U.K., Mar. 2015, pp. 173037-MS-1–173037-MS-12.

[32] C. Sagert, F. Di Meglio, M. Krstic, and P. Rouchon, "Backstepping and flatness approaches for stabilization of the stick-slip phenomenon for drilling," in *Proc. 5th Symp. Syst. Struct. Control*, Grenoble, France, Feb. 2013, pp. 779–784.

[33] E. Navarro-López and E. Licéaga-Castro, "Non-desired transitions and sliding-mode control of a multi-DOF mechanical system with stick-slip oscillations," *Chaos, Solitons Fract.*, vol. 41, no. 4, pp. 2035–2044, 2009.

[34] M. K. Johannessen and T. Myrvold, "Stick-slip prevention of drill strings using nonlinear model reduction and nonlinear model predictive control," M.S. thesis, Dept. Eng. Cybern., Norwegian Univ. Sci. Technol., Trondheim, Norway, 2010.

[35] C. Canudas-de-Wit, F. R. Rubio, and M. A. Corchero, "D-OSKIL: A new mechanism for controlling stick-slip oscillations in oil well drillstrings," *IEEE Trans. Control Syst. Technol.*, vol. 16, no. 6, pp. 1177–1191, Nov. 2008.

[36] T. Vromen, C.-H. Dai, N. van de Wouw, T. Oomen, P. Astrid, and H. Nijmeijer, "Robust output-feedback control to eliminate stick-slip oscillations in drill-string systems," in *Proc. 2nd IFAC Workshop Autom. Control Offshore Oil Gas Prod.*, Florianópolis, Brazil, May 2015, pp. 272–277.

[37] A. Kyllingstad and P. J. Nessjøen, "A new stick-slip prevention system," in *Proc. SPE/IADC Drilling Conf. Exhib.*, Amsterdam, The Netherlands, Mar. 2009, pp. 173042-MS-1–173042-MS-15

[38] R. Grauwmans and I. Stulemeijer, "Drilling efficiency optimization: Vibration study," in *Proc. Internal Present. Shell Exploration Prod.*, Rijswijk, The Netherlands, Dec. 2009.

[39] T. G. M. Vromen, "Control of stick-slip vibrations in drilling systems," Ph.D. dissertation, Dept. Mech. Eng., Eindhoven Univ. Technol., Eindhoven, The Netherlands, 2015. [Online]. Available: http://repository.tue.nl/59d54bcd-35f4-47d2-9ad1-033abfa51f83

[40] S. Skogestad and I. Postlethwaite, *Multivariable Feedback Control*, 2nd ed. Hoboken, NJ, USA: Wiley, 2005.

[41] K. Zhou, J. C. Doyle, and K. Glover, *Robust and Optimal Control*. Englewood Cliffs, NJ, USA: Prentice-Hall, 1996.

[42] T. Oomen, R. van Herpen, S. Quist, M. van de Wal, O. H. Bosgra, and M. Steinbuch, "Connecting system identification and robust control for next-generation motion control of a wafer stage," *IEEE Trans. Control Syst. Technol.*, vol. 22, no. 1, pp. 102–118, Jan. 2014.

[43] H. K. Khalil, *Nonlinear Systems*, 3rd ed. Englewood Cliffs, NJ, USA: Prentice-Hall, 2002.

[44] G. Meinsma, "Unstable and nonproper weights in H_∞ control," *Automatica*, vol. 31, no. 11, pp. 1655–1658, 1995.

Thijs Vromen was born in 1987. He received the M.Sc. degree (with Hons.) in mechanical engineering, and the Ph.D. degree from the Eindhoven University of Technology, Eindhoven, The Netherlands, in 2011 and 2015, respectively, where his thesis focused on control of stick-slip vibrations in drilling systems.

He is currently a Mechatronic Design Engineer with Océ Technologies, a Canon Company, Venlo, The Netherlands, where he is involved in the design of the paper transport system of cutsheet inkjet production printing systems.

Cam-Hing Dai received the M.Sc. degree in mechanical engineering with a specialization in dynamics and control from the Eindhoven University of Technology, Eindhoven, The Netherlands, in 2015.

He is currently with DAF Trucks N.V. (a heavy duty truck industry), a division of PACCAR Inc., Eindhoven, as a Control Function Design Engineer, where he is developing innovative engine software functionalities to meet future regulations, and increase the transport efficiency for its customers in the logistics industry.

Nathan van de Wouw (M'09) was born in 1970. He received the M.Sc. degree (with Hons.) and the Ph.D. degree in mechanical engineering from the Eindhoven University of Technology, Eindhoven, The Netherlands, in 1994 and 1999, respectively.

He is currently a Full Professor with the Mechanical Engineering Department, Eindhoven University of Technology, an Adjunct Full Professor with the University of Minnesota, Minneapolis, MN, USA, and a Full Professor (part-time) with the Delft University of Technology, Delft, The Netherlands. He was with Philips Applied Technologies, Eindhoven, and with the Netherlands Organization for Applied Scientific Research, Delft, in 2000 and 2001, respectively. He was a Visiting Professor at the University of California Santa Barbara, Santa Barbara, CA, USA, from 2006 to 2007, at The University of Melbourne, Melbourne, VIC, Australia, from 2009 to 2010, and at the University of Minnesota, from 2012 to 2013. He has authored a large number of journal and conference papers, and the books "Uniform Output Regulation of Nonlinear Systems: A convergent Dynamics Approach" with A.V. Pavlov and H. Nijmeijer (Birkhauser, 2005) and "Stability and Convergence of Mechanical Systems with Unilateral Constraints" with R.I. Leine (Springer-Verlag, 2008). His current research interests include the modeling analysis and control of nonlinear/hybrid systems, with applications to vehicular platooning, high-tech systems, resource exploration, smart energy systems, and networked control systems.

Dr. Wouw is currently an Associate Editor of *Automatica* and the IEEE TRANSACTIONS ON CONTROL SYSTEMS TECHNOLOGY. In 2015, he was a recipient of the IEEE Control Systems Technology Award "For the development and application of variable-gain control techniques for high-performance motion systems."

Tom Oomen (M'06) received the M.Sc. (*cum laude*) and Ph.D. degrees from the Eindhoven University of Technology, Eindhoven, The Netherlands.

He held visiting positions at KTH, Stockholm, Sweden, and at The University of Newcastle, Callaghan, NSW, Australia. Currently, he is an Assistant Professor with the Department of Mechanical Engineering, Eindhoven University of Technology. His current research interests include system identification, robust control, and learning control, with applications in mechatronic systems.

Dr. Oomen was a recipient of the Corus Young Talent Graduation Award, the 2015 IEEE TRANSACTIONS ON CONTROL SYSTEMS TECHNOLOGY Outstanding Paper Award, and the 2017 IFAC Mechatronics Best Paper Award. He is an Associate Editor of the IEEE Conference Editorial Board, *IFAC Mechatronics*, and the IEEE CONTROL SYSTEMS LETTERS.

Patricia Astrid (S'00–M'04) received the B.Eng. degree in engineering physics from the Bandung Institute of Technology, Bandung, Indonesia, in 1998, the M.Sc. degree in chemical engineering from the University of Groningen, Groningen, The Netherlands, in 2000, and the Ph.D. degree in control systems from the Department of Electrical Engineering, Eindhoven University of Technology, Eindhoven, The Netherlands, in 2004.

She was a Visiting Ph.D. Student at the Aerospace Computational Design Laboratory, Massachusetts Institute of Technology, Cambridge, MA, USA, in 2003. She joined Royal Dutch Shell, Rijswikj, The Netherlands, in 2006, involved in model reduction development to accelerate reservoir modeling simulation and advanced process control tool development for Shell's Downstream assets, where she is currently a Drilling Automation Project Lead and responsible for end-to-end development of autonomous drilling and well stimulation for Shell operations. Her current research interests include data-based modeling, large-scale model reduction and applications of machine learning, and artificial intelligence in energy industry.

Dr. Astrid is a reviewer for the IEEE CONTROL SYSTEMS TECHNOLOGY and the IEEE TRANSACTIONS OF AUTOMATIC CONTROL.

Apostolos Doris was born in Greece in 1976. He received the M.Sc. degree in mechanical engineering from the Aristotle University of Thessaloniki, Thessaloniki, Greece, in 2002, and the Ph.D. degree in mechanical engineering with a specialization in controller design for nonsmooth mechanical systems from the Technical University of Eindhoven, Eindhoven, The Netherlands, in 2007.

Since 2008, he has been a Research and Development Engineer, Life Cycle Engineer, Drilling Supervisor, and Project Leader with Shell, Rijswikj, The Netherlands. His current research interests include vibration suppression of drill-string systems, metal forming process of steel tubulars, and design, and implementation and operation of offshore wells.

Henk Nijmeijer (F'00) was born in 1955.

He is a Full Professor with the Eindhoven University of Technology, Eindhoven, The Netherlands, where he is also the Chair of the Dynamics and Control Group. He has authored a large number of journal and conference papers, and several books, and is or was at the editorial board of numerous journals. Mr. Nijmeijer is an Editor of *Communications in Nonlinear Science and Numerical Simulations*. He is appointed Honorary Knight of the "Golden Feedback Loop" (Norwegian University of Science and Technology) in 2011. Since 2011, he has been an IFAC Council Member. In 2015, he was the Scientific Director of the Dutch Institute of Systems and Control, Delft, The Netherlands. He is a Program Leader of the Dutch research program "Integrated Cooperative Automated Vehicles." Since 2017, he has been the Director of the Graduate Program Automotive Technology, Eindhoven University of Technology. He was a recipient of the 1990 IEE Heaviside premium and the 2015 IEEE Control Systems Technology Award.